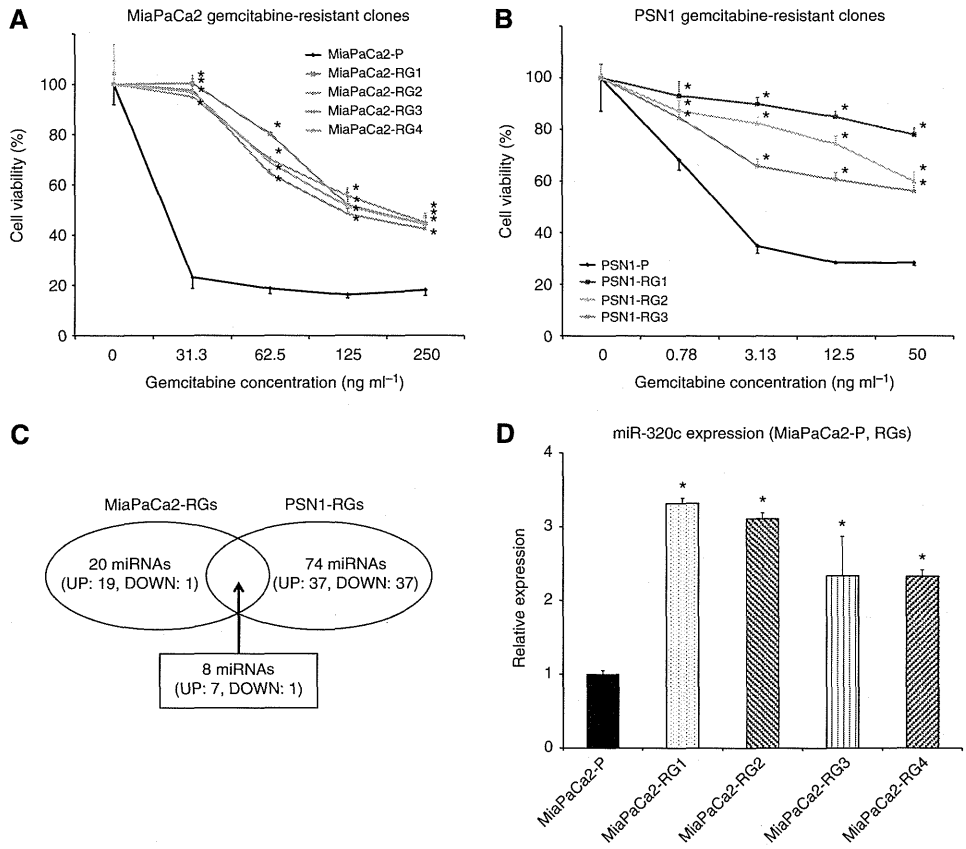

Figure 1. Characteristics of gemcitabine-resistant MiaPaCa2 cell clones (MiaPaCa2-RGs) and PSN1 cell clones (PSN1-RGs). (**A**, **B**) MTT assay showed significantly lower antitumour effect of gemcitabine in MiaPaCa2-RGs than in parental MiaPaCa2 cells (MiaPaCa2-P) and in PSN1-RGs than in parental PSN1 cells (PSN1-P). Data are mean ± s.d. of triplicate independent experiments. *$P<0.05$ compared with parental cells. (**C**) Schematic diagram of the results of microarray analysis. The protocol identified eight miRNAs in common with >1.5 average fold relative to parental, keeping adequate expression quantities and excluding miRNA*s both in MiaPaCa2-RGs and PSN1-RGs. (**D**) Real-time qRT–PCR demonstrated significantly higher miR-320c expression in MiaPaCa2-RGs than in MiaPaca2-P. Data are mean ± s.d. of triplicate independent experiments. *$P<0.05$.

Table 1. Common up- or downregulated miRNAs both in MiaPaCa2-RGs and PSN1-RGs

		Fold change (relative to MiaPaCa2-P)		Fold change (relative to PSN1-P)		
miR no.	Fold change (average)	MiaPaCa2-RGs (average)	P-value	PSN1-RGs (average)	*P*-value	Ref sequence ID
Common upregulated miRNAs both in MiaPaCa2-RGs and PSN1-RGs						
hsa-miR-320c	1.97	2.20	0.0033	1.73	0.0366	MIMAT0005793
hsa-miR-29a	1.85	2.13	0.0097	1.57	0.2751	MIMAT0000086
hsa-miR-10a	1.69	1.64	0.0202	1.73	0.0606	MIMAT0000253
hsa-miR-30c	1.68	1.54	0.0222	1.81	0.0384	MIMAT0000244
hsa-miR-30a	1.65	1.51	0.0243	1.79	0.2634	MIMAT0000087
hsa-miR-29b	1.58	1.53	0.0026	1.63	0.3311	MIMAT0000100
hsa-miR-320a	1.56	1.51	0.0142	1.61	0.0556	MIMAT0000510
Common downregulated miRNAs both in MiaPaCa2-RGs and PSN1-RGs						
hsa-miR-1246	3.65	1.97	0.0085	5.32	0.1209	MIMAT0005898

Abbreviations: MiaPaCa-P = parental MiaPaCa2 cells; MiaPaCa2-RGs = gemcitabine-resistant clones of MiaPaCa2; miR and miRNA = microRNA; PSN1-P = parental PSN1 cells; PSN1-RGs = gemcitabine-resistant clones of PSN1.

(Figure 2C). To further assess the effect of miR-320c on the gemcitabine resistance, anti-miR-320c was transfected into MiaPaCa2-RG1. Real-time qRT-PCR showed sufficient inhibition of miR-320c expression for over 72 h (Figure 2B), and the MTT assay demonstrated significant reduction of viability of anti-miR-320c-transfected cells compared with the control cells (Figure 2D). These results indicate that, at least partially, miR-320c induces gemcitabine resistance in MiaPaCa2 cells.

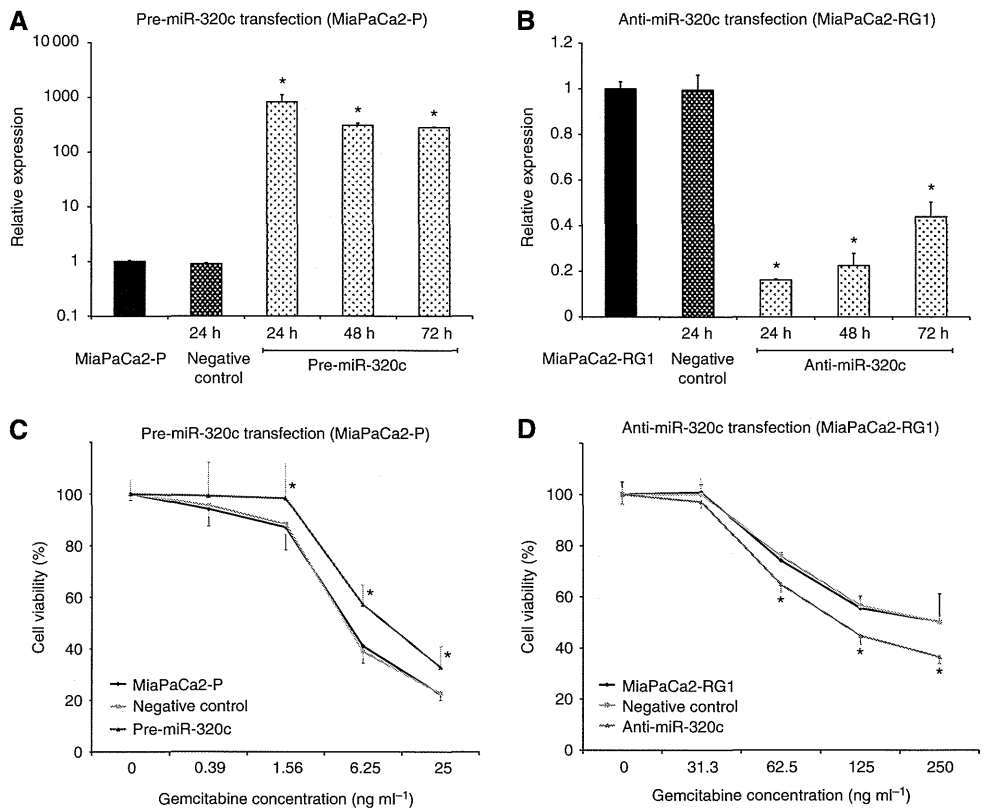

Figure 2. miR-320c induced gemcitabine resistance in MiaPaCa2 cells. (**A**, **B**) Real-time qRT-PCR confirmed overexpression (MiaPaCa2-P transfected with pre-miR-320c) and suppression (MiaPaCa2-RG1 transfected with anti-miR-320c) of miR-320c for >72 h. (**C**, **D**) MTT assay showed significant changes in resistance to gemcitabine by gain-of-function of miR-320c in MiaPaCa2-P and loss-of-function in MiaPaCa2-RG1. Data are mean ± s.d. of triplicate independent experiments. *$P<0.05$.

miR-320c inhibits the response to gemcitabine by targeting SMARCC1. Few studies have reported miR-320 expression in gastrointestinal cancers, and little is known about the function of this miRNA. As putative targets of miR-320c, 539 genes were predicted by TargetScan. Among them, SMARCC1, a component of the chromatin remodeling complex, also known as a tumour suppressor, was selected for further analysis. SMARCC1 expression was lower in MiaPaCa2-RG1 than in MiaPaCa2-P (Figure 3A). We investigated direct binding of miR-320c and the SMARCC1 gene by luciferase assay in MiaPaCa2-P and observed reduction of the luciferase activity in the pre-miR-320c-treated cells in comparison with negative control (Supplementary Figure S1). Pre-miR-320c transfection decreased SMARCC1 expression, and anti-miR-320c transfection increased it (Figures 3B and C), suggesting that SMARCC1 is one of the target genes of miR-320c in MiaPaCa2 cells. Next, we used siRNA for SMARCC1 to validate its involvement in the resistance to gemcitabine. Knockdown of SMARCC1 was confirmed by western blot analysis (Figure 3D). The MTT assay demonstrated that transfection of siSMARCC1 enhanced the resistance of MiaPaCa2-P to gemcitabine (Figure 3E). These results suggest that SMARCC1 mediates, at least in part, the miR-320c-related resistance to gemcitabine.

SMARCC1 expression in clinical pancreatic cancer samples. Pancreatic cancer samples of 66 patients who underwent R0 resection were immunohistochemically stained for SMARCC1 expression. Whereas the expression of SMARCC1 in pancreatic cancer lesions varied among the patients, a homogeneous staining for SMARCC1 was observed in the nucleus in normal pancreatic duct cells (Figure 4A). Although SMARCC1 has shown to appear not only in the nucleus but also in the cytoplasm in the previous study (Andersen *et al*, 2009), functional SMARCC1 protein is considered to localise in the nucleus, therefore we defined SMARCC1-positive samples as having the spotted granular nuclear pattern (Figure 4B) and SMARCC1-negative samples as having the cytoplasmic pattern (not stained in the nucleus) (Figure 4C) or the negative pattern (not stained in the nucleus or the cytoplasm) (Figure 4D) in pancreatic cancer lesions. Among the 66 patients examined, 31 (47.0%) showed positive staining whereas 35 (53.0%) patients were negative for SMARCC1.

SMARCC1 expression was not associated with overall and disease-free survival. Of all the 66 patients, the median overall survival was 17.0 months (3.5–147.7), and the median disease-free survival was 11.1 months (2.0–147.7). There were no significant differences between the groups who were SMARCC1 expression positive and negative with respect to age, sex, histopathological type (well/mod/poor), tumour size, tumour location (head/body/tail), pathological depth of tumour (pT1/T2/T3), and whether or not gemcitabine was used as chemotherapy. However, pathological lymph node metastasis and pathological stage were significantly different in the two groups ($P=0.0383$, $P=0.0383$, respectively) (Supplementary Table S4). The Kaplan–Meier overall survival estimates were not significantly different for patients who were SMARCC1 positive compared with those with SMARCC1-negative expression (median overall survival: 1.693 *vs* 2.189 years, $P=0.5585$; Supplementary Figure S2A). With regard to disease-free survival, there was no significant difference between the SMARCC1-positive and -negative groups (median disease-free survival, 0.956 *vs* 1.334 years, $P=0.5633$; Supplementary Figure S2B).

SMARCC1 was a useful predictor of clinical response to gemcitabine therapy. Of the 66 patients, 26 received therapy with single-agent gemcitabine. In 23 patients, this treatment was

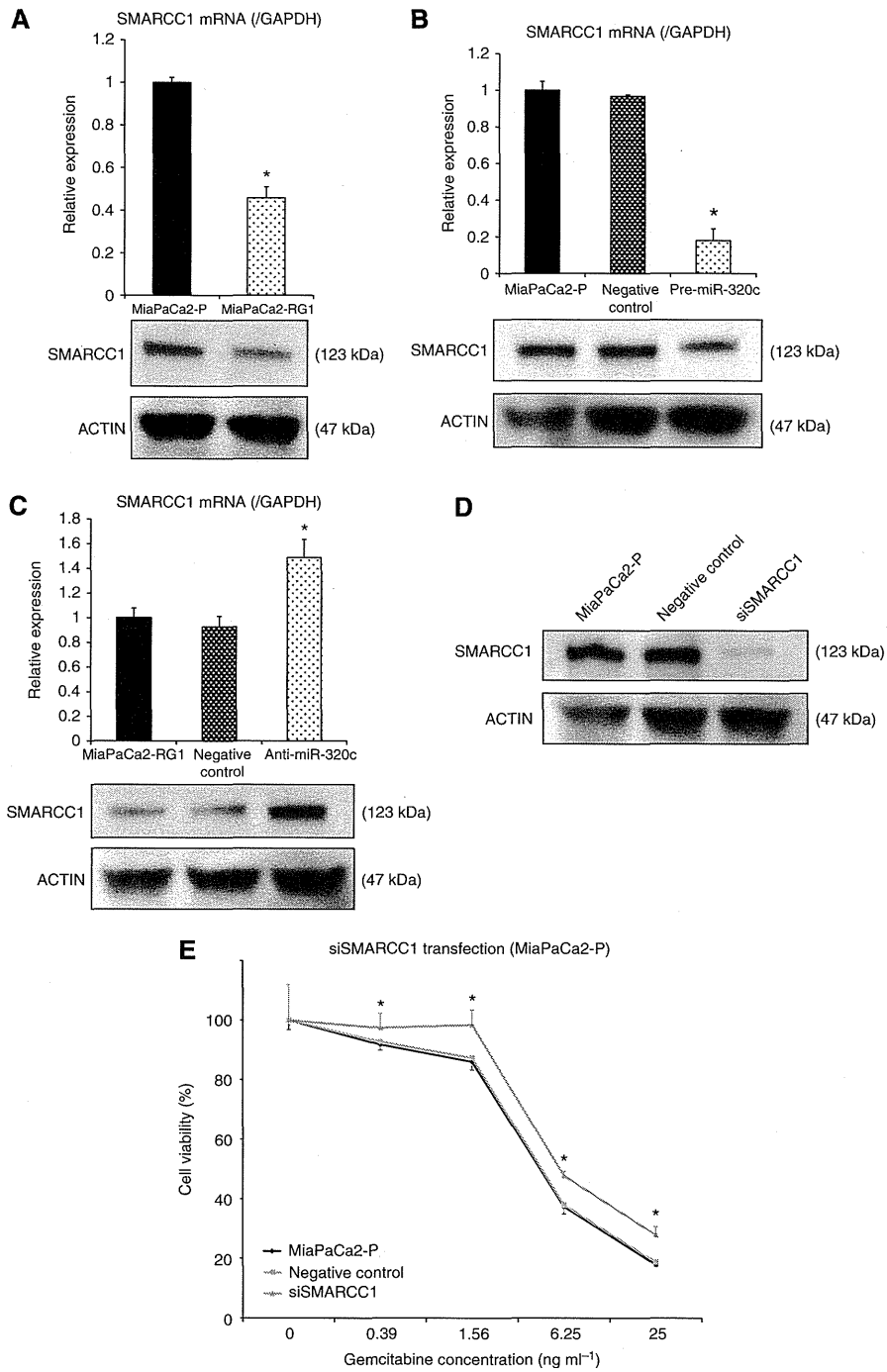

Figure 3. The miR-320c–related resistance to gemcitabine treatment is mediated through SMARCC1. (**A**) Real-time qRT-PCR and western blot analysis confirmed the significantly low SMARCC1 expression in MiaPaCa2-RG1 compared with MiaPaCa2-P. (**B**) SMARCC1 gene and protein expression was confirmed to be significantly suppressed by pre-miR-320c transfection in real-time qRT-PCR and western blot analysis. (**C**) real-time qRT-PCR and western blot analysis showed enhancement of SMARCC1 gene and protein expression levels by anti-miR-320c transfection. (**D**) Knockdown of SMARCC1 in MiaPaCa2-P was confirmed in western blot analysis. (**E**) MTT assay showed that knockdown of SMARCC1 induced resistance to gemcitabine treatment. Data are mean ± s.d. of triplicate independent experiments. *$P<0.05$.

initiated at the time of tumour recurrence. To elucidate the relationship between SMARCC1 expression and gemcitabine therapy, we used survival after recurrence, which represented the period from starting gemcitabine therapy or other therapies in 51 patients with relapse, until death. There were no significant differences between patients with and without gemcitabine therapy in clinicopathological factors (Table 2). First, we examined the survival benefit of gemcitabine. The 23 patients who were treated with gemcitabine had a significantly better survival than those who did not ($P=0.0046$; Supplementary Figure S3). After dividing patients who were treated with gemcitabine into SMARCC1-positive and -negative groups, only patients who were SMARCC1 positive benefited from gemcitabine therapy ($P=0.0463$). The relationship between SMARCC1 and survival after recurrence was not significant in patients treated without gemcitabine therapy ($P=0.9095$; Figure 5).

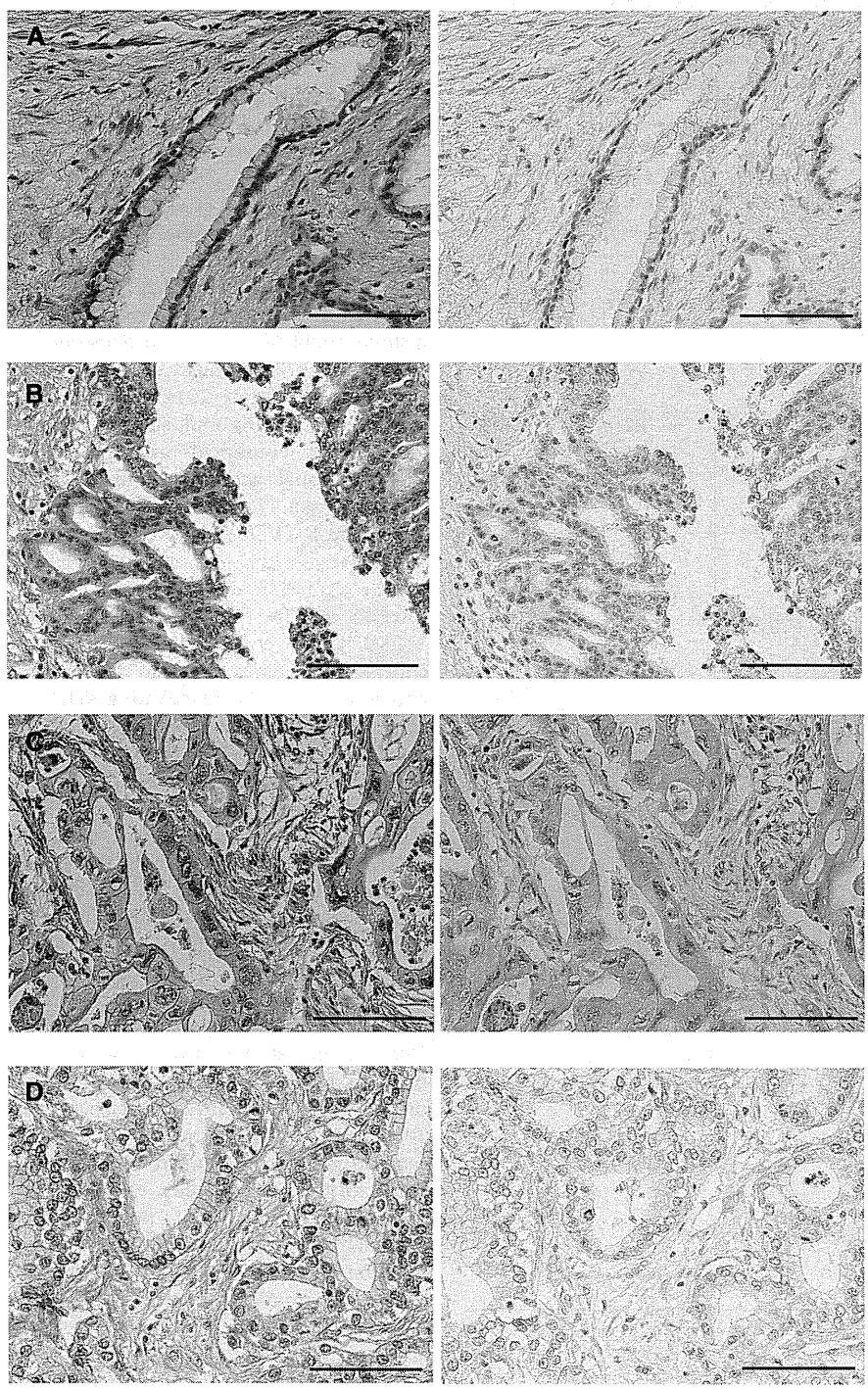

Figure 4. Immunohistochemistry for SMARCC1 in clinical samples. (A–D) Haematoxylin and eosin staining on the left side and SMARCC1 staining on the right side. **(A)** A normal pancreatic duct sample. SMARCC1 expression was identified in the nucleus homogeneously in normal pancreatic duct cells. **(B)** A representative SMARCC1-positive sample. SMARCC1 staining was in the spotted granular nuclear pattern in pancreatic carcinoma cells. **(C, D)** Representative SMARCC1-negative samples. SMARCC1 staining was in the cytoplasmic pattern (not stained in the nucleus) or in the negative pattern (not stained in the nucleus and the cytoplasm) in pancreatic carcinoma cells. Bar = 100 μm.

DISCUSSION

Several studies have examined the involvement of miR-320c in various types of cancer. It has been reported that miR-320c is upregulated in breast cancer (Yan *et al*, 2008), retinoblastoma (Zhao *et al*, 2009), and malignant transformed bronchial epithelial cells (Shen *et al*, 2009; Duan *et al*, 2010), whereas it is downregulated in lung cancer (Gao *et al*, 2011) and in cholangiocarcinoma (Chen *et al*, 2009). It has also been reported that miR-320 is regulated by PTEN in mammary stromal fibroblasts (Bronisz *et al*, 2012), correlates with recurrence-free survival in colon cancer (Schepeler *et al*, 2008), and inhibits proliferation in leukaemia (Schaar *et al*, 2009). Regarding the association of miR-320 and drug resistance, it has recently been reported that miR-320 facilitates chemotherapeutic drug-triggered apoptosis in cholangiocarcinoma (Chen *et al*, 2009). The present study identified miR-320c as one of the common upregulated

Table 2. Relationship between gemcitabine therapy and clinicopathological factors

	Gemcitabine therapy		
	Treated (n = 23)	**Not treated (n = 28)**	***P*-value**
Age (<65 : ⩾ 65 years)	13 : 10	12 : 16	0.3314
Sex (male:female)	11 : 12	14 : 14	0.8772
Histopathological type (well or mod:poor)	21 : 2	22 : 6	0.2134
Tumour size (<27 : ⩾27 mm)	12 : 11	12 : 16	0.5071
Tumour location (head:body or tail)	18 : 5	22 : 6	0.9786
Pathological depth of invasion pT (T1 or T2:T3)	2 : 21	1 : 27	0.4390
Pathological lymph node metastasis pN (negative:positive)	5 : 18	11 : 17	0.1790
Pathological stage (IA or IB or IIA:IIB or IV)	5 : 18	11 : 17	0.1790
SMARCC1 expression (−:+)	11 : 12	15 : 13	0.6830

Abbreviations: mod = moderately differentiated; poor = poorly differentiated; well = well differentiated.

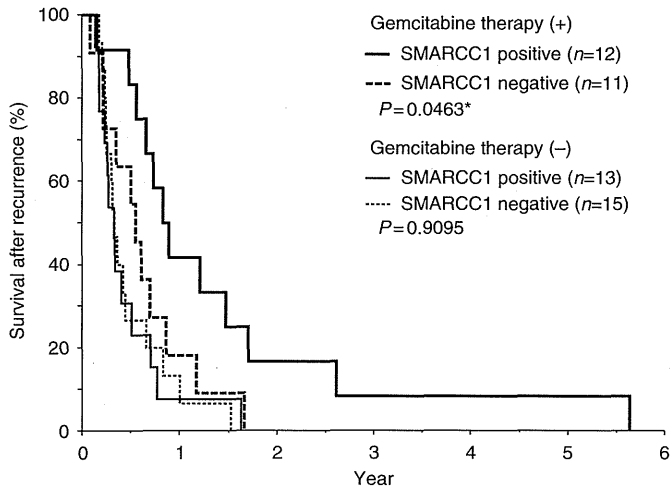

Figure 5. Relationship between SMARCC1 expression and survival after recurrence. Survival after recurrence curves showed a significantly better survival rate for SMARCC1-positive patients than for SMARCC1-negative patients treated with gemcitabine therapy (*$P = 0.0463$), but survival was not significantly different in patients treated without gemcitabine therapy ($P = 0.9095$).

miRNAs in gemcitabine-resistant pancreatic cancer cells compared with their parental cells, and we showed that miR-320c induced the resistance to gemcitabine. Among the putative targets of miR-320c by TargetScan, we focussed on SMARCC1, a switch/sucrose nonfermentable (SWI/SNF)-related matrix-associated actin-dependent regulator of chromatin subfamily C member 1, also known as BAF155 (BRG1-associated factor 155), as a candidate molecule responsible for miR-320-mediated drug resistance because of recent studies suggesting a role of chromatin remodeling in some cancers. Drug resistance is the major cause of treatment failure in cancer, yet the multifactorial mechanisms responsible for resistance remain largely unknown. Recently, several studies reported the contribution of chromatin remodeling in drug resistance in various types of cancer, such as the DEK oncogene in melanoma (Khodadoust *et al*, 2009), remodeling and spacing factor 1 in ovarian cancer (Choi *et al*, 2009), enhancer of zeste homolog 2 in pancreatic cancer (Ougolkov *et al*, 2008), and chromatin remodeling at the topoisomerase II-beta promoter in neuroblastoma (Das *et al*, 2010). Unlike DNA mutations, which are essentially irreversible in cancer, chromatin alterations, including both histone modifications and nucleosome remodeling, are potentially reversible and thus might constitute attractive therapeutic targets (Wilson and Roberts, 2011). The SWI/SNF chromatin remodeling complex is a 2-Mda multisubunit complex first identified in yeast and highly conserved among eukaryotes (Peterson, 1996). Transcriptional activation and efficient transcription of genes require dynamic structural changes in chromatin, and the ATP-dependent SWI/SNF complex is involved in chromatin restructuring (Percipalle and Farrants, 2006).

The SWI/SNF chromatin remodeling complex consists of a catalytic ATPase subunit, core subunits, and variant subunits. SMARCC1 is contained in the core subunits. The SWI/SNF complexes have a widespread role in tumour suppression (Wilson and Roberts, 2011). Inactivating deletion and mutations in SWI/SNF subunits have been reported at high frequency in various cancers, such as SNF5 in rhabdoid tumours (Versteege *et al*, 1998), BAF180 and ARID1A in renal cell carcinoma (Varela *et al*, 2011), ARID1A (Jones *et al*, 2010; Wiegand *et al*, 2010) and BAF155 (DelBove *et al*, 2011) in ovarian carcinoma, and BRG1, BRM, ARID1A, ARID1B, and BAF180 in pancreatic cancer (Shain *et al*, 2012). In addition, some SWI/SNF subunit deficiencies correlate with malignant potential, including drug resistance and shorter survival in melanoma (Lin *et al*, 2009) and in ovarian carcinoma (Katagiri *et al*, 2012) and glucocorticoid resistance in acute lymphoblastic leukaemia (Pottier *et al*, 2008), and as a severe risk factor for histologically malignant gastric cancer (Yamamichi *et al*, 2007). Some studies have reported that SMARCC1 deficiency prevents DNA damage–induced cell death (Ahn *et al*, 2011) and predicts short-term survival of colorectal cancer (Andersen *et al*, 2009). In addition, knockdown of SMARCC1 promotes self-renewal gene expression in embryonic stem cells (Schaniel *et al*, 2009). In the present study, we used MiaPaCa2-P and MiaPaCa2-RG1 and showed that knockdown of SMARCC1 induced gemcitabine resistance, and both gain-of-function and loss-of-function of miR-320c inversely altered the expression level of SMARCC1 protein. Although SMARCC1 may be only one of the responsible molecules, the molecule is shown to be involved, at least partly, in the miR-320c-related drug-resistance.

Evaluating the expression of miR-320c in clinical specimens may be crucial in predicting the drug-resistance, yet SMARCC1 may be practically easier and more useful than miR-320c. Thus, in the present study, we evaluated the clinical importance of SMARCC1 rather than miR-320c. We have previously reported RRM1 expression as the beneficial predictor of the clinical response to gemcitabine in pancreatic cancer patients after a complete resection (Akita *et al*, 2009). The present study revealed a significant association between SMARCC1 expression and the clinical response to gemcitabine therapy in completely resected pancreatic cancer patients. Therefore, RRM1, the key enzyme involved in DNA synthesis, and SMARCC1, the core subunit of the SWI/SNF chromatin remodeling complex, appear to make a contribution to drug-resistance mechanisms in separate processes and not to depend on each other. SMARCC1 expression could be a newly independent predictor of the clinical response to gemcitabine in pancreatic cancer patients.

In conclusion, we demonstrated in the present study that miR-320c inhibited the anti-cancer effect of gemcitabine in pancreatic cells and that SMARCC1 mediated this effect. The response to gemcitabine in MiaPaCa2 cells was controlled by genetic manipulation of miR-320c and SMARCC1. In addition, clinical examination revealed that only patients who were SMARCC1 positive benefited from gemcitabine therapy with regard to survival after recurrence. Considered together, the results suggest that miR-320c/SMARCC1-mediated gemcitabine resistance is a potential legitimate target for the treatment of pancreatic cancer.

ACKNOWLEDGEMENTS

We thank Nariaki Matsuura (Department of Molecular Pathology, Graduate School of Medicine, Osaka University, Osaka, Japan) for advice on immunohistochemical analysis.

CONFLICT OF INTEREST

The authors declare no conflict of interest.

REFERENCES

Ahn J, Ko M, Lee C, Kim J, Yoon H, Seong RH (2011) Srg3, a mouse homolog of BAF155, is a novel p53 target and acts as a tumor suppressor by modulating p21(WAF1/CIP1) expression. *Oncogene* **30**(4): 445–456.

Akita H, Zheng Z, Takeda Y, Kim C, Kittaka N, Kobayashi S, Marubashi S, Takemasa I, Nagano H, Dono K, Nakamori S, Monden M, Mori M, Doki Y, Bepler G (2009) Significance of RRM1 and ERCC1 expression in resectable pancreatic adenocarcinoma. *Oncogene* **28**(32): 2903–2909.

Ali S, Ahmad A, Banerjee S, Padhye S, Dominiak K, Schaffert JM, Wang Z, Philip PA, Sarkar FH (2010) Gemcitabine sensitivity can be induced in pancreatic cancer cells through modulation of miR-200 and miR-21 expression by curcumin or its analogue CDF. *Cancer Res* **70**(9): 3606–3617.

Andersen CL, Christensen LL, Thorsen K, Schepeler T, Sorensen FB, Verspaget HW, Simon R, Kruhoffer M, Aaltonen LA, Laurberg S, Orntoft TF (2009) Dysregulation of the transcription factors SOX4, CBFB and SMARCC1 correlates with outcome of colorectal cancer. *Br J Cancer* **100**(3): 511–523.

Bronisz A, Godlewski J, Wallace JA, Merchant AS, Nowicki MO, Mathsyaraja H, Srinivasan R, Trimboli AJ, Martin CK, Li F, Yu L, Fernandez SA, Pecot T, Rosol TJ, Cory S, Hallett M, Park M, Piper MG, Marsh CB, Yee LD, Jimenez RE, Nuovo G, Lawler SE, Chiocca EA, Leone G, Ostrowski MC (2012) Reprogramming of the tumour microenvironment by stromal PTEN-regulated miR-320. *Nat Cell Biol* **14**(2): 159–167.

Chen L, Yan HX, Yang W, Hu L, Yu LX, Liu Q, Li L, Huang DD, Ding J, Shen F, Zhou WP, Wu MC, Wang HY (2009) The role of microRNA expression pattern in human intrahepatic cholangiocarcinoma. *J Hepatol* **50**(2): 358–369.

Choi JH, Sheu JJ, Guan B, Jinawath N, Markowski P, Wang TL, Shih IeM (2009) Functional analysis of 11q13.5 amplicon identifies Rsf-1 (HBXAP) as a gene involved in paclitaxel resistance in ovarian cancer. *Cancer Res* **69**(4): 1407–1415.

Das CM, Zage PE, Taylor P, Aguilera D, Wolff JE, Lee D, Gopalakrishnan V (2010) Chromatin remodelling at the topoisomerase II-beta promoter is associated with enhanced sensitivity to etoposide in human neuroblastoma cell lines. *Eur J Cancer* **46**(15): 2771–2780.

Davidson JD, Ma L, Flagella M, Geeganage S, Gelbert LM, Slapak CA (2004) An increase in the expression of ribonucleotide reductase large subunit 1 is associated with gemcitabine resistance in non-small cell lung cancer cell lines. *Cancer Res* **64**(11): 3761–3766.

DelBove J, Rosson G, Strobeck M, Chen J, Archer TK, Wang W, Knudsen ES, Weissman BE (2011) Identification of a core member of the SWI/SNF complex, BAF155/SMARCC1, as a human tumor suppressor gene. *Epigenetics* **6**(12): 1444–1453.

Duan H, Jiang Y, Zhang H, Wu Y (2010) MiR-320 and miR-494 affect cell cycles of primary murine bronchial epithelial cells exposed to benzo[a]pyrene. *Toxicol In Vitro* **24**(3): 928–935.

Eguchi H, Nagano H, Yamamoto H, Miyamoto A, Kondo M, Dono K, Nakamori S, Umeshita K, Sakon M, Monden M (2000) Augmentation of antitumor activity of 5-fluorouracil by interferon alpha is associated with up-regulation of p27Kip1 in human hepatocellular carcinoma cells. *Clin Cancer Res* **6**(7): 2881–2890.

Gao W, Shen H, Liu L, Xu J, Shu Y (2011) MiR-21 overexpression in human primary squamous cell lung carcinoma is associated with poor patient prognosis. *J Cancer Res Clin Oncol* **137**(4): 557–566.

Giovannetti E, Funel N, Peters GJ, Del Chiaro M, Erozenci LA, Vasile E, Leon LG, Pollina LE, Groen A, Falcone A, Danesi R, Campani D, Verheul HM, Boggi U (2010) MicroRNA-21 in pancreatic cancer: correlation with clinical outcome and pharmacologic aspects underlying its role in the modulation of gemcitabine activity. *Cancer Res* **70**(11): 4528–4538.

Goan YG, Zhou B, Hu E, Mi S, Yen Y (1999) Overexpression of ribonucleotide reductase as a mechanism of resistance to 2,2-difluorodeoxycytidine in the human KB cancer cell line. *Cancer Res* **59**(17): 4204–4207.

Hwang JH, Voortman J, Giovannetti E, Steinberg SM, Leon LG, Kim YT, Funel N, Park JK, Kim MA, Kang GH, Kim SW, Del Chiaro M, Peters GJ, Giaccone G (2010) Identification of microRNA-21 as a biomarker for chemoresistance and clinical outcome following adjuvant therapy in resectable pancreatic cancer. *PloS One* **5**(5): e10630.

Ji Q, Hao X, Zhang M, Tang W, Yang M, Li L, Xiang D, Desano JT, Bommer GT, Fan D, Fearon ER, Lawrence TS, Xu L (2009) MicroRNA miR-34 inhibits human pancreatic cancer tumor-initiating cells. *PloS One* **4**(8): e6816.

Jones S, Wang TL, Shih IeM, Mao TL, Nakayama K, Roden R, Glas R, Slamon D, Diaz Jr. LA, Vogelstein B, Kinzler KW, Velculescu VE, Papadopoulos N (2010) Frequent mutations of chromatin remodeling gene ARID1A in ovarian clear cell carcinoma. *Science* **330**(6001): 228–231.

Katagiri A, Nakayama K, Rahman MT, Rahman M, Katagiri H, Nakayama N, Ishikawa M, Ishibashi T, Iida K, Kobayashi H, Otsuki Y, Nakayama S, Miyazaki K (2012) Loss of ARID1A expression is related to shorter progression-free survival and chemoresistance in ovarian clear cell carcinoma. *Mod Pathol* **25**(2): 282–288.

Khodadoust MS, Verhaegen M, Kappes F, Riveiro-Falkenbach E, Cigudosa JC, Kim DS, Chinnaiyan AM, Markovitz DM, Soengas MS (2009) Melanoma proliferation and chemoresistance controlled by the DEK oncogene. *Cancer Res* **69**(16): 6405–6413.

Kondo M, Yamamoto H, Nagano H, Okami J, Ito Y, Shimizu J, Eguchi H, Miyamoto A, Dono K, Umeshita K, Matsuura N, Wakasa K, Nakamori S, Sakon M, Monden M (1999) Increased expression of COX-2 in nontumor liver tissue is associated with shorter disease-free survival in patients with hepatocellular carcinoma. *Clin Cancer Res* **5**(12): 4005–4012.

Li D, Xie K, Wolff R, Abbruzzese JL (2004) Pancreatic cancer. *Lancet* **363**(9414): 1049–1057.

Li Y, VandenBoom 2nd TG, Kong D, Wang Z, Ali S, Philip PA, Sarkar FH (2009) Up-regulation of miR-200 and let-7 by natural agents leads to the reversal of epithelial-to-mesenchymal transition in gemcitabine-resistant pancreatic cancer cells. *Cancer Res* **69**(16): 6704–6712.

Lin H, Wong RP, Martinka M, Li G (2009) Loss of SNF5 expression correlates with poor patient survival in melanoma. *Clin Cancer Res* **15**(20): 6404–6411.

Nakahira S, Nakamori S, Tsujie M, Takahashi Y, Okami J, Yoshioka S, Yamasaki M, Marubashi S, Takemasa I, Miyamoto A, Takeda Y, Nagano H, Dono K, Umeshita K, Sakon M, Monden M (2007) Involvement of ribonucleotide reductase M1 subunit overexpression in gemcitabine resistance of human pancreatic cancer. *Int J Cancer* **120**(6): 1355–1363.

Oettle H, Post S, Neuhaus P, Gellert K, Langrehr J, Ridwelski K, Schramm H, Fahlke J, Zuelke C, Burkart C, Gutberlet K, Kettner E, Schmalenberg H, Weigang-Koehler K, Bechstein WO, Niedergethmann M, Schmidt-Wolf I, Roll L, Doerken B, Riess H (2007) Adjuvant chemotherapy with gemcitabine vs observation in patients undergoing curative-intent resection of pancreatic cancer: a randomized controlled trial. *JAMA* **297**(3): 267–277.

Ougolkov AV, Bilim VN, Billadeau DD (2008) Regulation of pancreatic tumor cell proliferation and chemoresistance by the histone methyltransferase enhancer of zeste homologue 2. *Clin Cancer Res* **14**(21): 6790–6796.

Park JK, Lee EJ, Esau C, Schmittgen TD (2009) Antisense inhibition of microRNA-21 or -221 arrests cell cycle, induces apoptosis, and sensitizes

the effects of gemcitabine in pancreatic adenocarcinoma. *Pancreas* **38**(7): e190–e199.
Percipalle P, Farrants AK (2006) Chromatin remodelling and transcription: be-WICHed by nuclear myosin 1. *Curr Opin Cell Biol* **18**(3): 267–274.
Peterson CL (1996) Multiple SWItches to turn on chromatin? *Curr Opin Genet Dev* **6**(2): 171–175.
Pottier N, Yang W, Assem M, Panetta JC, Pei D, Paugh SW, Cheng C, Den Boer ML, Relling MV, Pieters R, Evans WE, Cheok MH (2008) The SWI/SNF chromatin-remodeling complex and glucocorticoid resistance in acute lymphoblastic leukemia. *J Natl Cancer Inst* **100**(24): 1792–1803.
Schaar DG, Medina DJ, Moore DF, Strair RK, Ting Y (2009) miR-320 targets transferrin receptor 1 (CD71) and inhibits cell proliferation. *Exp Hematol* **37**(2): 245–255.
Schaniel C, Ang YS, Ratnakumar K, Cormier C, James T, Bernstein E, Lemischka IR, Paddison PJ (2009) Smarcc1/Baf155 couples self-renewal gene repression with changes in chromatin structure in mouse embryonic stem cells. *Stem Cells* **27**(12): 2979–2991.
Schepeler T, Reinert JT, Ostenfeld MS, Christensen LL, Silahtaroglu AN, Dyrskjot L, Wiuf C, Sorensen FJ, Kruhoffer M, Laurberg S, Kauppinen S, Orntoft TF, Andersen CL (2008) Diagnostic and prognostic microRNAs in stage II colon cancer. *Cancer Res* **68**(15): 6416–6424.
Schmittgen TD, Jiang J, Liu Q, Yang L (2004) A high-throughput method to monitor the expression of microRNA precursors. *Nucleic Acids Res* **32**(4): e43.
Shain AH, Giacomini CP, Matsukuma K, Karikari CA, Bashyam MD, Hidalgo M, Maitra A, Pollack JR (2012) Convergent structural alterations define SWItch/Sucrose NonFermentable (SWI/SNF) chromatin remodeler as a central tumor suppressive complex in pancreatic cancer. *Proc Natl Acad Sci USA* **109**(5): E252–E259.
Shen YL, Jiang YG, Greenlee AR, Zhou LL, Liu LH (2009) MicroRNA expression profiles and miR-10a target in anti-benzo[a] pyrene-7, 8-diol-9, 10-epoxide-transformed human 16HBE cells. *Biomed Environ Sci* **22**(1): 14–21.
Tomimaru Y, Eguchi H, Nagano H, Wada H, Tomokuni A, Kobayashi S, Marubashi S, Takeda Y, Tanemura M, Umeshita K, Doki Y, Mori M (2010) MicroRNA-21 induces resistance to the anti-tumour effect of interferon-alpha/5-fluorouracil in hepatocellular carcinoma cells. *Br J Cancer* **103**(10): 1617–1626.
Tomokuni A, Eguchi H, Tomimaru Y, Wada H, Kawamoto K, Kobayashi S, Marubashi S, Tanemura M, Nagano H, Mori M, Doki Y (2011) miR-146a suppresses the sensitivity to interferon-alpha in hepatocellular carcinoma cells. *Biochem Biophys Res Commun* **414**(4): 675–680.
Varela I, Tarpey P, Raine K, Huang D, Ong CK, Stephens P, Davies H, Jones D, Lin ML, Teague J, Bignell G, Butler A, Cho J, Dalgliesh GL, Galappaththige D, Greenman C, Hardy C, Jia M, Latimer C, Lau KW, Marshall J, McLaren S, Menzies A, Mudie L, Stebbings L, Largaespada DA, Wessels LF, Richard S, Kahnoski RJ, Anema J, Tuveson DA, Perez-Mancera PA, Mustonen V, Fischer A, Adams DJ, Rust A, Chan-on W, Subimerb C, Dykema K, Furge K, Campbell PJ, Teh BT, Stratton MR, Futreal PA (2011) Exome sequencing identifies frequent mutation of the SWI/SNF complex gene PBRM1 in renal carcinoma. *Nature* **469**(7331): 539–542.
Versteege I, Sevenet N, Lange J, Rousseau-Merck MF, Ambros P, Handgretinger R, Aurias A, Delattre O (1998) Truncating mutations of hSNF5/INI1 in aggressive paediatric cancer. *Nature* **394**(6689): 203–206.
Wiegand KC, Shah SP, Al-Agha OM, Zhao Y, Tse K, Zeng T, Senz J, McConechy MK, Anglesio MS, Kalloger SE, Yang W, Heravi-Moussavi A, Giuliany R, Chow C, Fee J, Zayed A, Prentice L, Melnyk N, Turashvili G, Delaney AD, Madore J, Yip S, McPherson AW, Ha G, Bell L, Fereday S, Tam A, Galletta L, Tonin PN, Provencher D, Miller D, Jones SJ, Moore RA, Morin GB, Oloumi A, Boyd N, Aparicio SA, Shih IeM, Mes-Masson AM, Bowtell DD, Hirst M, Gilks B, Marra MA, Huntsman DG (2010) ARID1A mutations in endometriosis-associated ovarian carcinomas. *N Engl J Med* **363**(16): 1532–1543.
Wilson BG, Roberts CW (2011) SWI/SNF nucleosome remodellers and cancer. *Nat Rev Cancer* **11**(7): 481–492.
Yamamichi N, Inada K, Ichinose M, Yamamichi-Nishina M, Mizutani T, Watanabe H, Shiogama K, Fujishiro M, Okazaki T, Yahagi N, Haraguchi T, Fujita S, Tsutsumi Y, Omata M, Iba H (2007) Frequent loss of Brm expression in gastric cancer correlates with histologic features and differentiation state. *Cancer Res* **67**(22): 10727–10735.
Yamamoto H, Kondo M, Nakamori S, Nagano H, Wakasa K, Sugita Y, Chang-De J, Kobayashi S, Damdinsuren B, Dono K, Umeshita K, Sekimoto M, Sakon M, Matsuura N, Monden M (2003) JTE-522, a cyclooxygenase-2 inhibitor, is an effective chemopreventive agent against rat experimental liver fibrosis1. *Gastroenterology* **125**(2): 556–571.
Yamamoto T, Nagano H, Sakon M, Wada H, Eguchi H, Kondo M, Damdinsuren B, Ota H, Nakamura M, Marubashi S, Miyamoto A, Dono K, Umeshita K, Nakamori S, Yagita H, Monden M (2004) Partial contribution of tumor necrosis factor-related apoptosis-inducing ligand (TRAIL)/TRAIL receptor pathway to antitumor effects of interferon-alpha/5-fluorouracil against hepatocellular carcinoma. *Clin Cancer Res* **10**(23): 7884–7895.
Yan LX, Huang XF, Shao Q, Huang MY, Deng L, Wu QL, Zeng YX, Shao JY (2008) MicroRNA miR-21 overexpression in human breast cancer is associated with advanced clinical stage, lymph node metastasis and patient poor prognosis. *RNA* **14**(11): 2348–2360.
Yang MH, Chen CL, Chau GY, Chiou SH, Su CW, Chou TY, Peng WL, Wu JC (2009) Comprehensive analysis of the independent effect of twist and snail in promoting metastasis of hepatocellular carcinoma. *Hepatology* **50**(5): 1464–1474.
Zhang XJ, Ye H, Zeng CW, He B, Zhang H, Chen YQ (2010) Dysregulation of miR-15a and miR-214 in human pancreatic cancer. *J Hematol Oncol* **3**: 46.
Zhao JJ, Yang J, Lin J, Yao N, Zhu Y, Zheng J, Xu J, Cheng JQ, Lin JY, Ma X (2009) Identification of miRNAs associated with tumorigenesis of retinoblastoma by miRNA microarray analysis. *Childs Nerv Syst* **25**(1): 13–20.

Supplementary Information accompanies this paper on British Journal of Cancer website (http://www.nature.com/bjc)

Leukemia Research 37 (2013) 21–27

Contents lists available at SciVerse ScienceDirect

Leukemia Research

journal homepage: www.elsevier.com/locate/leukres

Angioimmunoblastic T-cell lymphoma mice model

Fumihiko Sato[a,b], Takashi Ishida[a,*], Asahi Ito[a], Fumiko Mori[a], Ayako Masaki[a], Hisashi Takino[b], Tomoko Narita[a], Masaki Ri[a], Shigeru Kusumoto[a], Susumu Suzuki[c], Hirokazu Komatsu[a], Akio Niimi[a], Ryuzo Ueda[c], Hiroshi Inagaki[b], Shinsuke Iida[a]

[a] Department of Medical Oncology and Immunology, Nagoya City University Graduate School of Medical Sciences, 1 Kawasumi, Mizuho-chou, Mizuho-ku, Nagoya, Aichi 467-8601, Japan
[b] Department of Anatomic Pathology and Molecular Diagnostics, Nagoya City University Graduate School of Medical Sciences, 1 Kawasumi, Mizuho-chou, Mizuho-ku, Nagoya, Aichi 467-8601, Japan
[c] Department of Tumor Immunology, Aichi Medical University School of Medicine, Nagakute, Aichi 480-1195, Japan

ARTICLE INFO

Article history:
Received 7 May 2012
Received in revised form 26 July 2012
Accepted 11 September 2012
Available online 29 September 2012

Keywords:
Angioimmunoblastic T-cell lymphoma
Follicular helper T cell
BCL6
PD1
NOG mice
Tumor microenvironment

ABSTRACT

We established an angioimmunoblastic T-cell lymphoma (AITL) mouse model using NOD/Shi-*scid*, IL-2Rγ^{null} mice as recipients. The immunohistological findings of the AITL mice were almost identical to those of patients with AITL. In addition, substantial amounts of human immunoglobulin G/A/M were detected in the sera of the AITL mice. This result indicates that AITL tumor cells helped antibody production by B cells or plasma cells. This is the first report of reconstituting follicular helper T (TFH) function in AITL cells in an experimental model, and this is consistent with the theory that TFH cell is the cell of origin of AITL tumor cells.

1. Introduction

Angioimmunoblastic T-cell lymphoma (AITL) represents a distinct clinicopathological entity among nodal peripheral T-cell lymphomas. A complex network of interactions between AITL tumor cells and the various reactive cellular components of the tumor microenvironment forms the clinical and histological features of AITL [1]. Because of its complexity, analysis of the immunopathogenesis of AITL in vitro seems to be impossible. On the other hand, recent advances in the development of novel mouse models, in which human hematopoietic and/or immune systems could be reconstituted, have contributed to analyzing the pathogenesis of various human diseases and evaluating the effects of therapeutic agents [2–6]. In the present study, we aimed to establish a novel AITL mouse model in which both primary tumor cells of human AITL and microenvironmental reactive cells engraft and interact with each other, using NOD/Shi-*scid*, IL-2Rγ^{null} (NOG) mice [7,8] as recipients, and analyzed the immunopathogenesis of AITL.

2. Materials and methods

2.1. Human cells

The donors of tumor cells provided written informed consent before sampling in accordance with the Declaration of Helsinki. The present study was approved by the institutional ethics committee of Nagoya City University Graduate School of Medical Sciences.

2.2. Animals

NOG mice were purchased from the Central Institute for Experimental Animals and used at 6–8 weeks of age. All of the in vivo experiments were performed in accordance with the United Kingdom Coordinating Committee on Cancer Research Guidelines for the Welfare of Animals in Experimental Neoplasia, Second Edition, and were approved by the ethics committee of the Center for Experimental Animal Science, Nagoya City University Graduate School of Medical Sciences.

2.3. Primary AITL cell-bearing mouse model

The affected lymph node cells from two patients with AITL were suspended in RPMI-1640, and intraperitoneally (i.p.) injected into NOG mice. Lymph node cells of AITL patient 1 were injected at a dose of 2.5×10^7 lymph node cells/mouse (total 2 mice), and those of patient 2 were injected at a dose of 4.0×10^6 lymph node cells/mouse (total 3 mice). When mice that had received lymph node cells from patient 1 or 2 became weakened, they were sacrificed at day 34 and 48, respectively.

2.4. Antibodies and flow cytometry

The following antibodies were used for flow cytometry: MultiTEST CD3 (clone SK7) FITC/CD16 (B73.1)+CD56 (NCAM 16.2) PE/CD45 (2D1) PerCP/CD19 (SJ25C1)

* Corresponding author. Tel.: +81 52 853 8216; fax: +81 52 852 0849.
E-mail address: itakashi@med.nagoya-cu.ac.jp (T. Ishida).

0145-2126/$ – see front matter © 2012 Elsevier Ltd. All rights reserved.
http://dx.doi.org/10.1016/j.leukres.2012.09.009

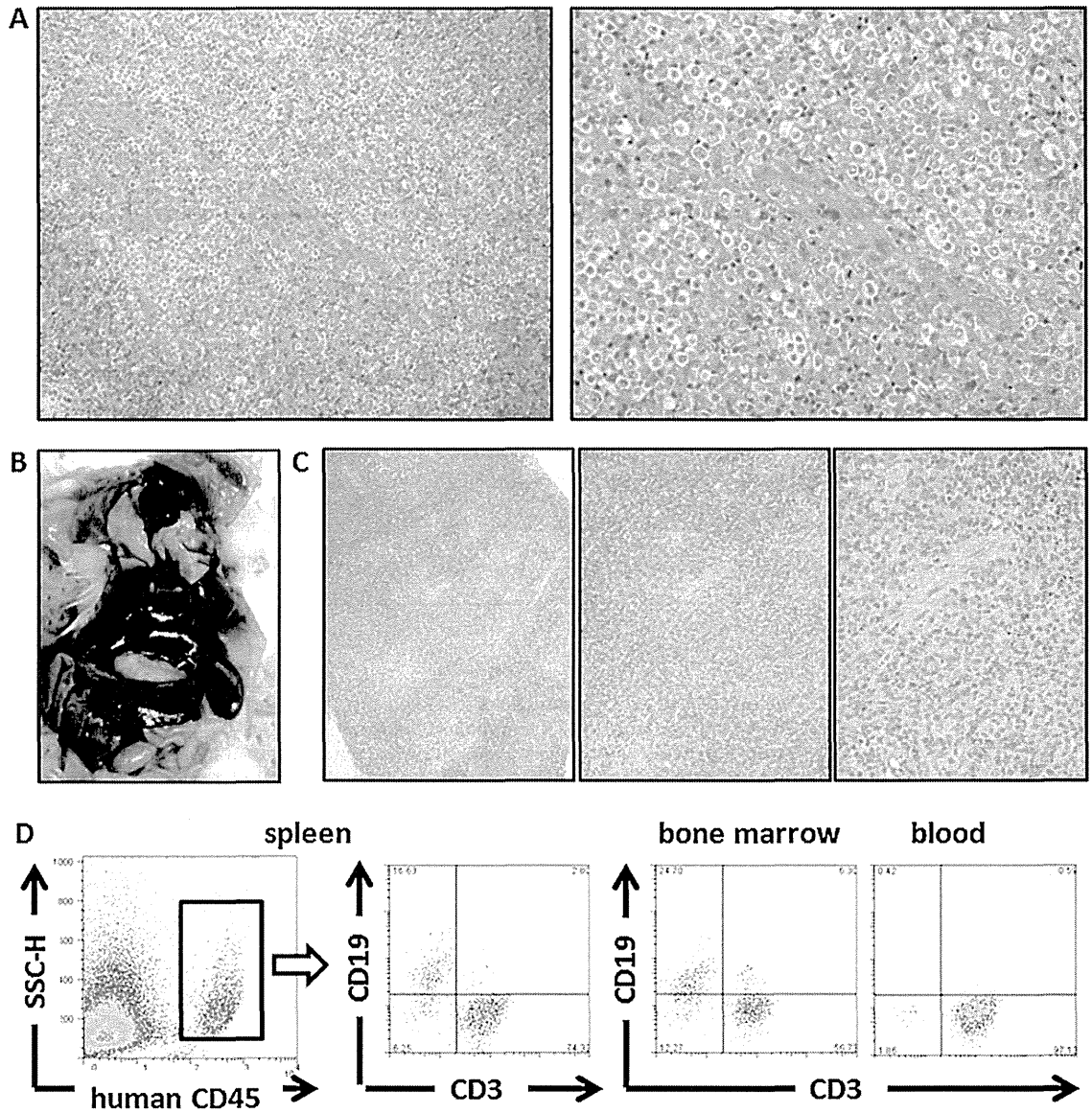

Fig. 1. Primary AITL cell-bearing NOG mouse model. (A) Microscopic images with hematoxylin and eosin staining of the affected lymph node of AITL patient 1 are shown. (B) Macroscopic image of a primary AITL cell-bearing NOG mouse is shown. (C) Sections of the AITL-affected mouse spleen with hematoxylin and eosin staining are shown. (D) The presence of human CD45-positive cells in the infiltrate of the mouse spleen, bone marrow, and blood was determined by flow cytometric analysis of human CD3 and CD19 expression.

APC Reagent, MultiTEST CD3 FITC/CD8 (SK1) PE/CD45 PerCP/CD4 (SK3) APC Reagent. All antibodies were purchased from BD Biosciences (San Jose, CA, USA). Whole blood cells from mice were treated with BD FACS lysing solution (BD Biosciences) for lysing red blood cells. Cells were analyzed by a FACSCalibur (BD Biosciences) with the aid of FlowJo software (Tree Star, Inc., Ashland, OR, USA).

2.5. Immunopathological analysis

Hematoxylin and eosin (HE) staining and immunostaining using antihuman alpha-smooth muscle actin (α-SMA) (1A4; DAKO, Glostrup, Denmark), VEGF-A (sc-152, rabbit polyclonal, Santa Cruz, Heidelberg, Germany), CD3 (SP7; SPRING BIOSCIENCE, Pleasanton, CA, USA), CD20 (L26; DAKO), PD1 (programmed death 1, CD279) (ab52587, Abcam, Cambridge, MA, USA), CD138 (B-B4, Serotec, Raleigh, NC, USA), B cell lymphoma 6 (BCL6) (EP529Y; Epitomics, Burlingame, CA, USA), CD45RO (UCHL1, DAKO), immunoglobulin kappa (KP-53, Novocastra, Newcastle, UK) and lambda light chain (HP-6054, Novocastra) were performed. The presence of Epstein–Barr virus encoded RNA (EBER) was examined by in situ hybridization using EBER Probe (Leica Microsystems, Newcastle, UK) on formalin-fixed, paraffin-embedded sections. Double immunostaining analysis of human CD45RO and human BCL6 was performed as previously described [9]. Briefly, formalin-fixed, paraffin-embedded sections of AITL-affected spleen were immunostained using antibodies against human CD45RO and human BCL6. CD45RO protein in the membrane was visualized in purple (Bajoran purple, Biocare Medical, Concord, CA, USA) and BCL6 protein in the nucleus was visualized in brown (DAB, Leica Microsystems).

2.6. Clonality assay

Clonal assessment of the AITL cells was performed using IdentiClone™ TCRB Gene Clonality Assay (*In vivo*Scribe Technologies, Inc., San Diego, CA, USA) according to the instructions of the manufacturer. Southern blotting analysis of T cell receptor Cβ1 gene was performed at SRL, Inc. (Tokyo, Japan).

2.7. Mouse serum protein

The mouse serum protein fraction was analyzed at SRL, Inc. Human immunoglobulin (Ig) G/A/M in mice serum were also measured at SRL, Inc.

3. Results

3.1. Establishment of the primary AITL cell-bearing NOG mouse model

Microscopic images of the affected lymph node of AITL patient 1 are shown in Fig. 1A. There was marked proliferation of arborizing

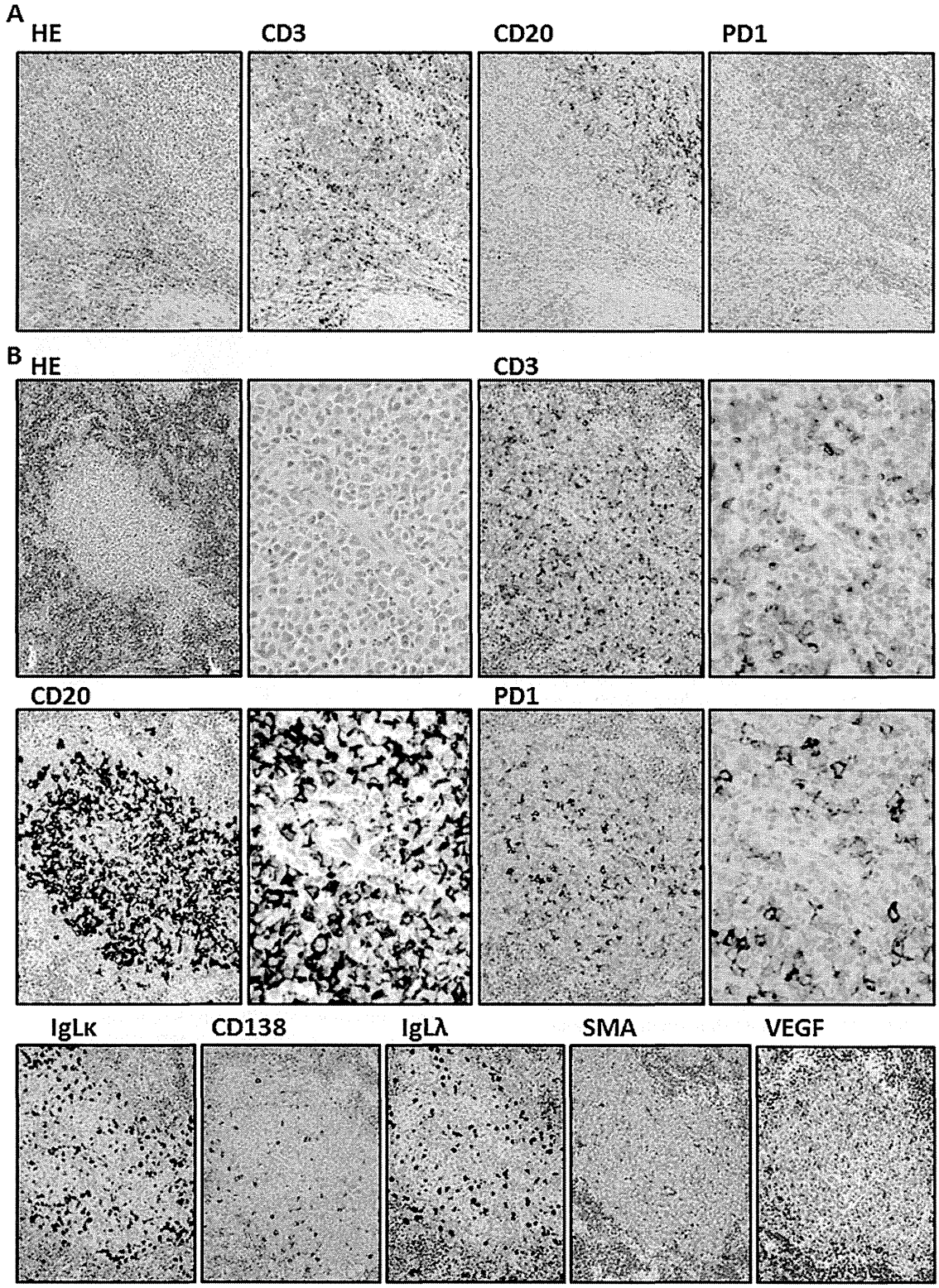

Fig. 2. Immunohistochemical analysis of primary AITL cell-bearing NOG mouse model. (A) Microscopic images with hematoxylin and eosin staining, and staining by anti-CD3, CD20, PD1, and CD138, of the affected lymph node of AITL patient 2 are shown. (B) Immunohistochemical images of sections of the spleen of a primary AITL-affected mouse that had been injected with affected lymph node cells from patient 2, with hematoxylin and eosin staining, and staining by anti-CD3, CD20, PD1, CD138, immunoglobulin kappa and lambda light chain, VEGF-A, and alpha-smooth muscle actin (α-SMA).

high endothelial venules (HEV). There was polymorphic infiltrate composed of small to medium-sized lymphocytes with clear to pale cytoplasm, distinct cell membranes and minimal cytological atypia. The neoplastic cells were admixed with variable numbers of small reactive lymphocytes, eosinophils, plasma cells, and histiocytes. These histological findings are typical of AITL [10]. NOG mice bearing AITL cells from patient 1 presented marked splenomegaly and mild hepatomegaly. The macroscopic appearance of a primary AITL cell-bearing NOG mouse from patient 1 is shown in Fig. 1B. Microscopic analysis revealed that the mice spleen

architectures were partially replaced by the infiltration of small to medium-sized lymphocytes with clear to pale cytoplasm, distinct cell membranes and minimal cytological atypia. The infiltrate also included plasma cells. Marked proliferation of HEV was seen in the spleen (Fig. 1C).

Flow cytometric analysis demonstrated that human CD3-positive T cells as well as CD19-positive B cells infiltrated into the spleen of the mice (Fig. 1D, left 2 panels). Both human T and B cells also infiltrated the mice bone marrow, but only T cells were detected in the blood (Fig. 1D, right 2 panels).

Microscopic images of the affected lymph node of AITL patient 2 are shown in Fig. 2A. There was polymorphic infiltrate composed of small to medium-sized lymphocytes including CD3-positive T cells as well as CD20-positive B cells. Some of the infiltrated cells were positive for PD1, which is known to be expressed on follicular helper T (TFH) cells [11,12] as well as AITL tumor cells [13]. These histological findings are also typical of AITL [10].

NOG mice bearing AITL cells from patient 2 presented marked splenomegaly and mild hepatomegaly. Immunohistochemical analyses of the AITL mice from patient 2 also demonstrated that the mice spleen architectures were partially replaced by the infiltration of small to medium-sized lymphocytes with clear to pale cytoplasm (Fig. 2B, upper left 2 panels). CD3-positive T cells (Fig. 2B, upper right 2 panels) as well as CD20-positive B cells (Fig. 2B, middle left 2 panels) infiltrated the mice spleen. Some of the infiltrated cells were positive for PD1 (Fig. 2B, middle right 2 panels). The infiltrated cells included CD138-positive plasma cells with no slanted distributions of immunoglobulin kappa or lambda light chain (Fig. 2B, lower left 3 panels). EBER-positive cells were not observed in the infiltrate (data not shown). There were abundant SMA-positive blood vessels in the spleen, and the infiltrate included VEGF-producing cells, most of which were AITL tumor cells (Fig. 2B, lower right 2 panels). These observations collectively indicated that the infiltrate consisted of PD1-positive AITL cells, a large number of reactive lymphocytes including both B and T cells, and polyclonal plasma cells, and there was marked vascular proliferation in the spleen. These immunohistological findings in the NOG AITL mice (Figs. 1C and 2B) were nearly identical to those in the respective donor AITL patients (Figs. 1A and 2A).

3.2. Human antibody production in the AITL NOG mice

Given the observation that there were abundant reactive human lymphocytes including B cells and plasma cells in AITL-affected mice spleen, we investigated whether they produced human Ig in the AITL NOG mice. As shown in Fig. 3A, significant Ig fractions and substantial amounts of human IgG/A/M were detected in the AITL mice from both donors. Double immunostaining revealed that human CD45RO- and BCL6-double-positive cells were detected in AITL-affected spleen (Fig. 3B). On the other hand, $CD45RO^{-}BCL6^{+}$ cells were considered to be reactive B cells, because BCL6 is a transcriptional repressor expressed by germinal center B cells [14,15]. These observations collectively indicated that $CD45RO^{+}BCL6^{+}$ AITL tumor cells helped antibody production by B cells or plasma cells. $CD45RO^{+}BCL6^{-}$ cells were also detected in the spleen, and they were reactive T cells with memory phenotype [16].

3.3. Serial transplantations in AITL NOG mice

Suspensions of spleen cells from the mice receiving primary lymph node cells from AITL patient 1 were serially i.p. transplanted into fresh NOG mice. The second NOG mice were sacrificed when they became weakened. The second NOG mice presented marked splenomegaly and mild hepatomegaly (data not shown). Flow cytometric analysis demonstrated that human CD3-positive T cells, including both CD4 and CD8 cells, infiltrated into the mice liver, spleen, and bone marrow. In contrast to the first AITL mice, infiltration of B cells (CD4 and CD8 double negative cells) was not observed (Fig. 4A, left 6 panels). In the subsequent 3rd AITL mice, infiltration of CD8 cells was markedly decreased, and in the 4th AITL mice, the infiltrate of the liver, spleen, and bone marrow consisted of almost exclusively CD4-positive T cells (Fig. 4A, right 6 panels). Along with the disappearance of infiltrating B cells, human Ig was not detected in the sera of 2nd, 3rd and 4th AITL NOG mice (Fig. 4B). Clonality analysis by PCR detected clonal rearrangement of the T cell receptor in the affected lymph node from AITL patient 1 (Fig. 4C, top panel), which was confirmed by Southern blotting analysis of the T cell receptor Cβ1 gene (Fig. 4D, left panels, arrows). Clonality analysis by PCR demonstrated that there were two T cell clones in the spleen cells of the first AITL NOG mice, and the product size of one of these two was the same as that of the original AITL patient (Fig. 4C, upper 2 panels, arrows), indicating that a neoplastic T cell clone from the original AITL patient engrafted and proliferated in the first AITL NOG mice. This observation was confirmed by Southern blotting analysis (Fig. 4D, arrows). The same two T cell clones were detected in the 3rd and 4th AITL mice as those in the 1st AITL mice (Fig. 4C, lower 3 panels, arrows and arrowheads).

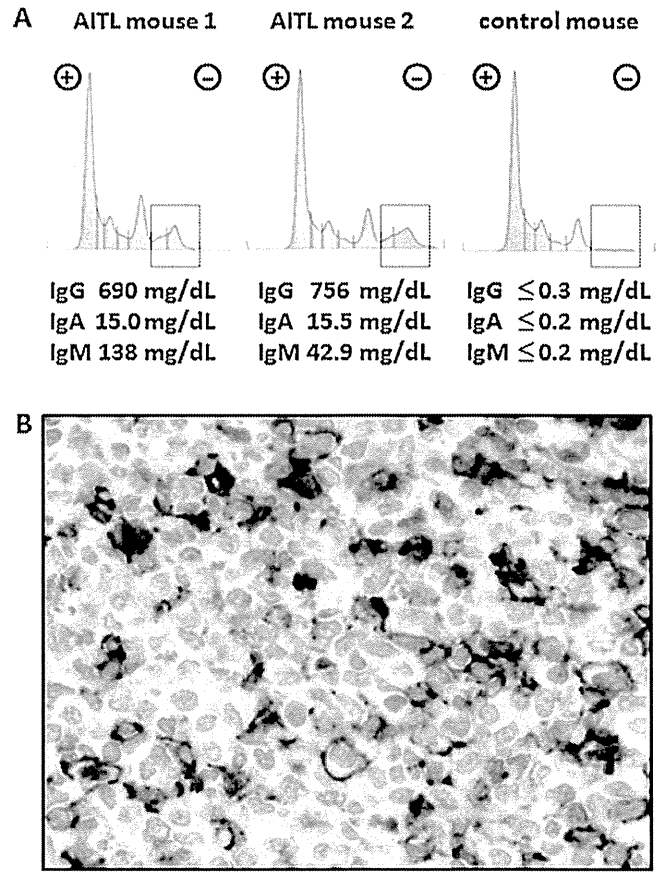

Fig. 3. Human antibody production in the AITL NOG mice. (A) Serum protein fraction of NOG mice that had been injected with affected lymph node cells from AITL patient 1 and 2, and that of a naïve NOG mouse. (B) Double immunostaining analysis for human CD45RO and BCL6 in the AITL-affected mouse spleen. CD45RO in the membrane is visualized in purple and BCL6 in the nucleus is visualized in brown.

3.4. Macroscopic and microscopic findings of 4th AITL mice

The 4th AITL mice presented marked splenomegaly and mild hepatomegaly (Fig. 5A). Mice spleen architectures were almost wholly replaced by the infiltration of small to medium-sized lymphocytes with clear to pale cytoplasm. There was also marked

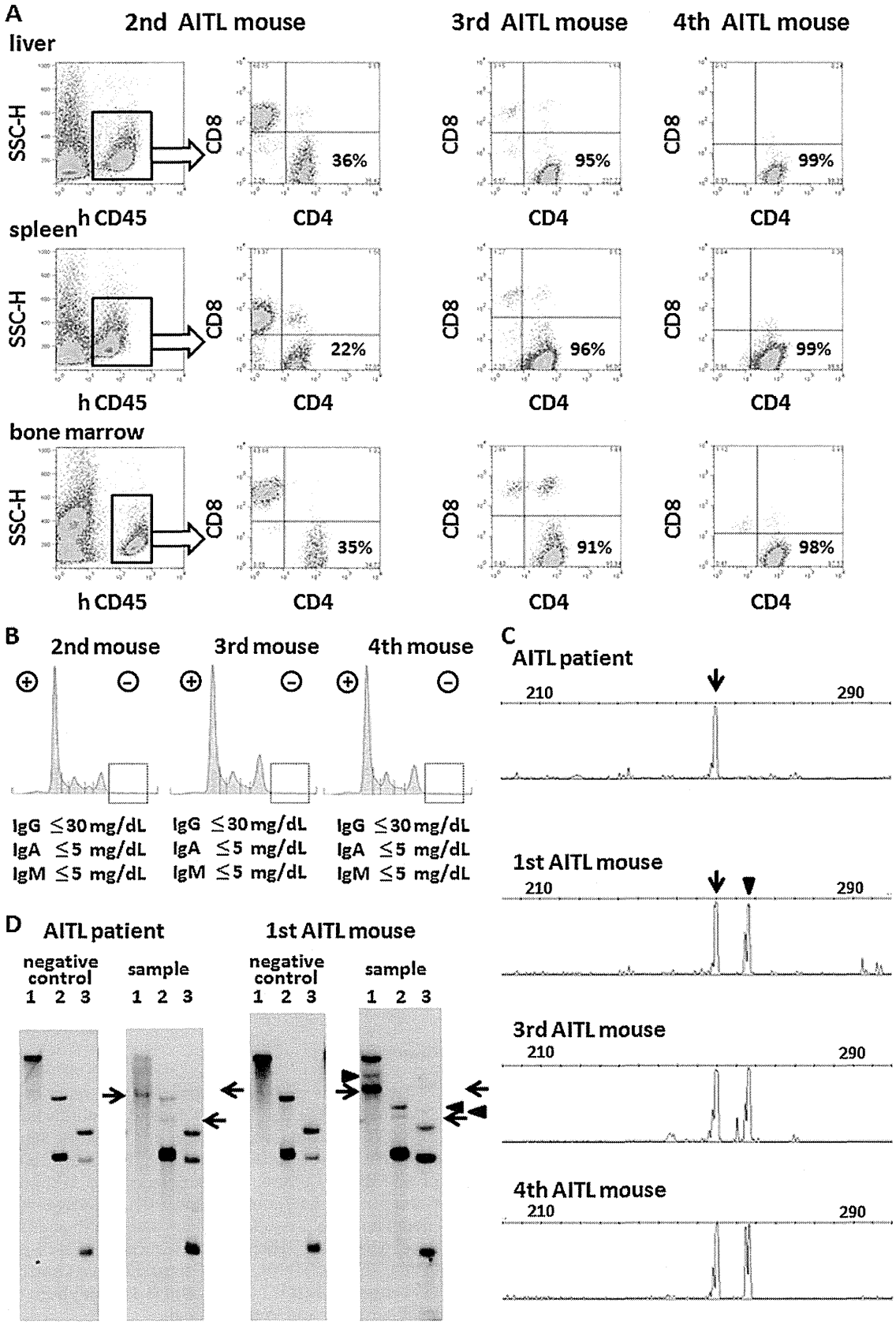

Fig. 4. Serial transplantations of spleen cells from AITL NOG mice. (A) The presence of human CD45-positive cells in the liver, spleen and bone marrow of the 2nd, 3rd, and 4th AITL NOG mice was determined by human CD4 and CD8 expression. (B) Serum protein fraction of 2nd, 3rd, and 4th AITL NOG mice. (C) Clonality analysis by PCR. Arrow and arrowhead indicate the clonal rearrangement of T cell receptor. (D) Clonality analysis by Southern blotting of T cell receptor Cβ1 gene. 1, 2, and 3 indicate BamH I, EcoR V, and Hind III, respectively. Arrow and arrowhead indicate the rearrangement band.

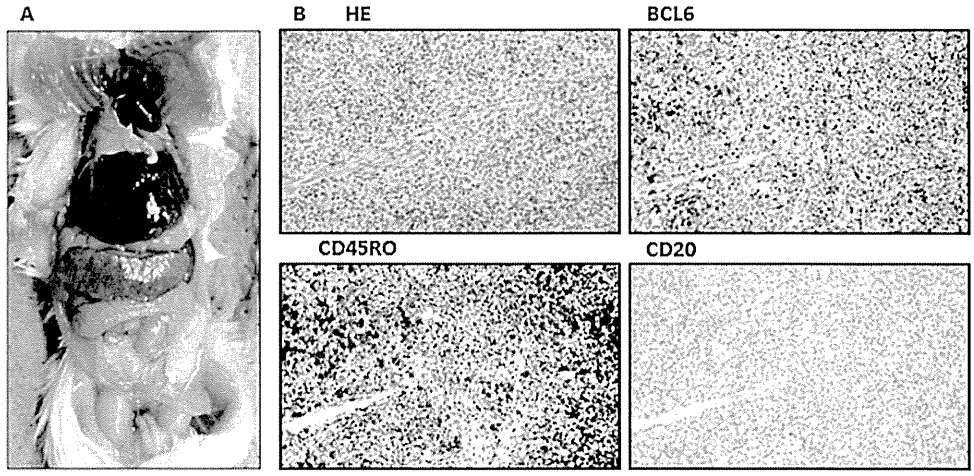

Fig. 5. Macroscopic and microscopic findings of 4th AITL mice. (A) Macroscopic image of a 4th AITL mouse. (B) Immunohistochemical images of the 4th AITL mouse spleen with hematoxylin and eosin staining, and staining by anti-BCL6, CD45RO, and CD20 antibodies.

vascular proliferation in the spleen. Most of the infiltrated cells were positive for CD45RO and BCL6. In contrast to the 1st AITL NOG mice, there were no CD20- (Fig. 5B) or CD138-positive reactive cells (data not shown), which were consistent with the results of flow cytometric analyses (Fig. 4A).

4. Discussion

The recent identification of $CD4^+$ TFH cell as the cell of origin of AITL provides a rationale to explain some of the clinical and histological features of AITL. A fundamental function of TFH cells is regulation of B cell-mediated humoral immunity. It has been known that in humanized NOG mice reconstituted with human $CD34^+$ hematopoietic stem cells, there was little IgG production because of the inappropriate differentiation of human B cells in the mouse environment [17–20]. Considering this fact, it was striking that the present AITL NOG mice produced polyclonal human Ig including IgG. This was direct evidence that $CD45RO^+BCL6^+$ AITL tumor cells functioned as TFH cells, and to the best of our knowledge, this is the first report to reconstitute TFH function in AITL cells in an experimental model either in vitro or in vivo. This could also explain one of the characteristic clinical features of AITL patients, hypergammaglobulinemia. In the AITL mice, human B cells were observed in the spleen and bone marrow, but not in blood, suggesting that antibody production mediated by T cells might need a suitable microenvironment like the germinal center of lymph nodes.

Serial transplantations of spleen cells of AITL NOG mice resulted in the reduction of reactive components such as B cell lineage and CD8-positive cells. CD4-positive AITL neoplastic cells can survive for a long period of time only by interacting with mouse environment cells. As a result, they failed to interact with human B or plasma cells, leading to the absence of human Ig production in the 2nd, 3rd, and 4th AITL NOG mice.

In general, not only monoclonal T cell receptor rearrangement, but also oligoclonal rearrangements were detected in AITL cases [1]. In the present study, although only one T cell clone (clone #1) was detected in an AITL patient 1, another T cell clone (clone #2) was also detected in the AITL NOG mice. We surmise that there were two neoplastic clones in the patient's affected lymph node, although the level of clone #2 was below the detectable limit. Because NOG mice have severe multiple immune dysfunctions, clone #2 was able to increase in the mice to a detectable level.

The immunohistological findings of the present AITL mice were almost identical to those of AITL patients; i.e., only a fraction of AITL neoplastic cells, which were small to medium-sized cells with clear cytoplasms and minimal cytologic atypia, were admixed with a reactive population of small lymphocytes including B and T cells, and plasma cells, and the spleen showed prominent vascularization. On the other hand, there was a lack of myeloid lineage cells such as eosinophils, histiocytes, and follicular dendritic cells, in the background inflammatory components, probably due to their fundamentally short life span. There was also a lack of EBV-positive B cells in the infiltrate in the present AITL mice, which could be explained by the fact that there was a lack of EBV-positive B cells in the background inflammatory components in the affected lymph node of both donors. In this type of analysis, attention should be paid to cross-reaction of antihuman antigens antibodies to mouse cells. The antihuman CD3, CD20, PD1, CD138, BCL6, CD45RO, immunoglobulin kappa and lambda light chain antibodies in the present study did not react with hematopoietic cells of mice origin (data not shown), probably due to the lack of mice T, B, and NK cells in NOG mice [7,8].

In conclusion, primary AITL tumor cells and reactive components engrafted NOG mice, and AITL cells interacted with B and plasma cells, and functioned as TFH cells. Human Igs including IgG were produced in the mice. The present observations strongly support the recent identification of TFH cell as the cell of origin of AITL. The present procedures using NOG mice would be a powerful tool to understand the immunopathogenesis of AITL.

Grants support

The present study was supported by Grants-in-Aid for Young Scientists (A) (No. 22689029, T. Ishida), Scientific Research (B) (No. 22300333, T. Ishida, and R. Ueda), and Scientific Support Programs for Cancer Research (No. 221S0001, T. Ishida) from the Ministry of Education, Culture, Sports, Science and Technology of Japan, Grants-in-Aid for National Cancer Center Research and Development Fund (No. 21-6-3, T. Ishida), and Health and Labour Sciences Research Grants (H22-Clinical Cancer Research-general-028, T. Ishida, and H23-Third Term Comprehensive Control Research for Cancer-general-011, T. Ishida, and H. Inagaki) from the Ministry of Health, Labour and Welfare, Japan.

Conflicts of interest

Nagoya City University Graduate School of Medical Sciences has received research grant support from Kyowa Hakko Kirin for works

provided by Takashi Ishida. No other conflict of interest relevant to this article is reported.

Acknowledgements

We thank Ms. Chiori Fukuyama for her excellent technical assistance, and Ms. Naomi Ochiai for her excellent secretarial assistance.

Authors' contributions. F.S., T.I., R.U., and H.I. designed the research. F.S., T.I., A.I., F.M., A.M., and H.T. performed the experiments. All of the authors analyzed and interpreted the data. F.S. and T.I. wrote the paper, and all of the other authors contributed to writing the paper.

References

[1] de Leval L, Gisselbrecht C, Gaulard P. Advances in the understanding and management of angioimmunoblastic T-cell lymphoma. Br J Haematol 2010;148:673–89.
[2] Barabe F, Kennedy JA, Hope KJ, Dick JE. Modeling the initiation and progression of human acute leukemia in mice. Science 2007;316:600–4.
[3] Ishikawa F, Yoshida S, Saito Y, Hijikata A, Kitamura H, Tanaka S, et al. Chemotherapy resistant human AML stem cells home to and engraft within the bone-marrow endosteal region. Nat Biotechnol 2007;25: 1315–21.
[4] Mori F, Ishida T, Ito A, Sato F, Masaki A, Takino H, et al. Potent antitumor effects of bevacizumab in a microenvironment-dependent human lymphoma mouse model. Blood Cancer J 2012;2:e67.
[5] Sato K, Misawa N, Nie C, Satou Y, Iwakiri D, Matsuoka M, et al. A novel animal model of Epstein–Barr virus-associated hemophagocytic lymphohistiocytosis in humanized mice. Blood 2011;117:5663–73.
[6] Ito A, Ishida T, Utsunomiya A, Sato F, Mori F, Yano H, et al. Defucosylated anti-CCR4 monoclonal antibody exerts potent ADCC against primary ATLL cells mediated by autologous human immune cells in NOD/Shi-scid, IL-2R gamma(null) mice in vivo. J Immunol 2009;183:4782–91.
[7] Ito M, Hiramatsu H, Kobayashi K, Suzue K, Kawahata M, Hioki K, et al. NOD/SCID/γcnull mouse: an excellent recipient mouse model for engraftment of human cells. Blood 2002;100:3175–82.
[8] Ito M, Kobayashi K, Nakahata T. NOD/Shi-scid IL2rγnull (NOG) mice more appropriate for humanized mouse models. Curr Top Microbiol Immunol 2008;324:53–76.
[9] Ishida T, Ishii T, Inagaki A, Yano H, Komatsu H, Iida S, et al. Specific recruitment of CC chemokine receptor 4-positive regulatory T cells in Hodgkin lymphoma fosters immune privilege. Cancer Res 2006;66:5716–22.
[10] Dogan A, Gaulard P, Jaffe ES, Ralfkiaer E, Muller-Hermelink HK. Angioimmunoblastic T-cell lymphoma. In: Swerdlow SH, Campo E, Harris NL, Jaffe ES, Pileri SA, Stein H, Thiele J, Vardiman JW, editors. WHO classification of tumours of haematopoietic and lymphoid tissues. Lyon: IARC; 2008. p. 309.
[11] Fazilleau N, McHeyzer-Williams LJ, Rosen H, McHeyzer-Williams MG. The function of follicular helper T cells is regulated by the strength of T cell antigen receptor binding. Nat Immunol 2009;10:375–84.
[12] Haynes NM, Allen CD, Lesley R, Ansel KM, Killeen N, Cyster JG. Role of CXCR5 and CCR7 in follicular Th cell positioning and appearance of a programmed cell death gene-1high germinal center-associated subpopulation. J Immunol 2007;179:5099–108.
[13] Roncador G, García Verdes-Montenegro JF, Tedoldi S, Paterson JC, Klapper W, Ballabio E, et al. Expression of two markers of germinal center T cells (SAP and PD-1) in angioimmunoblastic T-cell lymphoma. Haematologica 2007;92:1059–66.
[14] Crotty S, Johnston RJ, Schoenberger SP. Effectors and memories: Bcl-6 and Blimp-1 in T and B lymphocyte differentiation. Nat Immunol 2010;11:114–20.
[15] Klein U, Dalla-Favera R. Germinal centres: role in B-cell physiology and malignancy. Nat Rev Immunol 2008;8:22–33.
[16] Akbar AN, Terry L, Timms A, Beverley PC, Janossy G. Loss of CD45R and gain of UCHL1 reactivity is a feature of primed T cells. J Immunol 1988;140:2171–8.
[17] Ishikawa F, Yasukawa M, Lyons B, Yoshida S, Miyamoto T, Yoshimoto G, et al. Development of functional human blood and immune systems in NOD/SCID/IL2 receptor {gamma} chain(null) mice. Blood 2005;106:1565–73.
[18] Matsumura T, Kametani Y, Ando K, Hirano Y, Katano I, Ito R, et al. Functional CD5+ B cells develop predominantly in the spleen of NOD/SCID/gammac(null) (NOG) mice transplanted either with human umbilical cord blood, bone marrow, or mobilized peripheral blood CD34+ cells. Exp Hematol 2003;31:789–97.
[19] Traggiai E, Chicha L, Mazzucchelli L, Bronz L, Piffaretti JC, Lanzavecchia A, et al. Development of a human adaptive immune system in cord blood cell-transplanted mice. Science 2004;304:104–7.
[20] Watanabe Y, Takahashi T, Okajima A, Shiokawa M, Ishii N, Katano I, et al. The analysis of the functions of human B and T cells in humanized NOD/shi-scid/gammac(null) (NOG) mice (hu-HSC NOG mice). Int Immunol 2009;21:843–58.

Cancer Science
The official journal of the Japanese Cancer Association JCA

Case Report

Stevens–Johnson Syndrome associated with mogamulizumab treatment of adult T-cell leukemia/lymphoma

Takashi Ishida,[1,6] Asahi Ito,[1] Fumihiko Sato,[2] Shigeru Kusumoto,[1] Shinsuke Iida,[1] Hiroshi Inagaki,[2] Akimichi Morita,[3] Shiro Akinaga[4] and Ryuzo Ueda[5]

Departments of [1]Medical Oncology and Immunology, [2]Anatomic Pathology and Molecular Diagnostics, [3]Geriatric and Environmental Dermatology, Nagoya City University Graduate School of Medical Sciences, Nagoya; [4]Kyowa Hakko Kirin, Tokyo; [5]Department of Tumor Immunology, Aichi Medical University School of Medicine, Nagakute, Japan

(Received December 25, 2012/Revised January 21, 2013/Accepted January 23, 2013/Accepted manuscript online January 30, 2013)

We report an adult T-cell leukemia/lymphoma patient suffering from Stevens–Johnson Syndrome (SJS) during mogamulizumab (humanized anti-CCR4 monoclonal antibody) treatment. There was a durable significant reduction of the $CD4^+CD25^{high}FOXP3^+$ regulatory T (Treg) cell subset in the patient's PBMC, and the affected inflamed skin almost completely lacked FOXP3-positive cells. This implies an association between reduction of the Treg subset by mogamulizimab and occurrence of SJS. The present case should contribute not only to our understanding of human pathology resulting from therapeutic depletion of Treg cells, but also alert us to the possibility of immune-related severe adverse events such as SJS when using mogamulizumab. We are currently conducting a clinical trial of mogamulizumab for CCR4-negative solid cancers (UMIN000010050), specifically aiming to deplete Treg cells. (*Cancer Sci* 2013; 104: 647–650)

Adult T-cell leukemia/lymphoma (ATL) is an aggressive peripheral T-cell neoplasm caused by HTLV-1. The disease is resistant to conventional chemotherapeutic agents, and has a very poor prognosis.[1] Mogamulizumab (KW-0761) is a defucosylated humanized monoclonal antibody targeting CC chemokine receptor 4 (CCR4).[2] A phase I clinical trial for relapsed CCR4-positive peripheral T-cell neoplasms, including ATL, and a phase II study for relapsed ATL have been conducted with mogamulizumab.[3,4] This agent was subsequently approved for the treatment of relapsed or refractory ATL in Japan, the first country in the world to do so, in March 2012. Mogamulizimab went on sale on 29 May 2012. The interim report for the post-marketing surveillance from 29 May to 28 September 2012 revealed skin-related severe adverse events (SAE), as defined by the Medical Dictionary for Regulatory Activities Terminology/Japan, in nine patients. Thus, during only the first 4 months of use, 9 skin-related SAE, including 4 cases of Stevens–Johnson Syndrome (SJS)/toxic epidermal necrolysis (TEN) were reported, with 1 SJS/TEN fatality. These skin-related, potentially fatal SAE are certainly a challenge to the free use of this agent and clearly require investigation. Therefore, here we report an informative ATL patient suffering from SJS on mogamulizumab treatment, focusing on the reduction of the regulatory T (Treg) cell subset ($CD4^+CD25^{high}FOXP3^+$) caused by the antibody.

Case Report

A 71-year old woman was admitted due to elevation of her lymphocyte count. She had been diagnosed as suffering from acute-type ATL nearly 5 months prior to admission. She had received VCAP-AMP-VECP chemotherapy[5] followed by oral sobuzoxane in another hospital, and achieved a transient partial remission. We started mogamulizumab to treat the flare-up of ATL disease (Fig. 1). Grade 1 skin eruptions appeared around her neck after three antibody infusions. Because we were also giving her antibacterial (ciprofloxacin hydrochloride), fungal (itraconazole), pneumocystic (sulfamethoxazole-trimethoprim) and viral (aciclovir) prophylaxes in addition to stomach medicine (lansoprazole), we judged the skin event to be due to drug eruption caused by one of these concomitant drugs. Therefore, we stopped all five, but continued with mogamulizumab. Despite their discontinuation and treatment with topical steroids, the skin rashes continued to worsen. We started the patient on 30 mg oral prednisolone, which improved the skin symptoms. The patient was then able to complete the eight planned infusions, and oral prednisolone was tapered off. She was discharged from hospital 8 days after her eighth infusion (day 65), and thereafter seen as an outpatient. However, she had to be readmitted as an emergency patient at day 75 because of fulminant skin rashes. These included erythemas, scale-like plaques, vesicles, blisters and erosions over many areas of the body. Her lips were swollen and oral mucosa was erosive (Fig. 2a). Skin biopsy revealed marked liquefaction, degeneration and perivascular inflammation with dominant CD8-positive cells but almost complete lack of FOXP3-positive cells (Fig. 2b). We diagnosed her as a SJS, and immediately started steroid pulse therapy (methylprednisolone 500 mg/day ×3 days), followed by oral prednisolone. Her skin and mucosal lesions improved gradually, and became inactive. At the same time, her general condition improved. Thus, we again tapered the steroid dose, and she was discharged at day 144. However, she had to come back yet again as an emergency patient on day 151 for the same reason as before, with fulminant skin rashes. We prescribed her mini-steroid pulse therapy (methylprednisolone 125 mg/day ×1 day), followed by oral prednisolone. Once more, her skin lesions improved gradually. Over this whole period, complete ATL remission was maintained by mogamulizumab. The HTLV-1 provirus load in PBMC pre-treatment, and at days 121 and 162 was 750.1, 0.0 (under the limit of detection) and 0.8 copies/1000 cells, respectively. These post-treatment values are strikingly low, considering that median HTLV-1

[6]To whom correspondence should be addressed.
E-mail: itakashi@med.nagoya-cu.ac.jp

doi: 10.1111/cas.12116

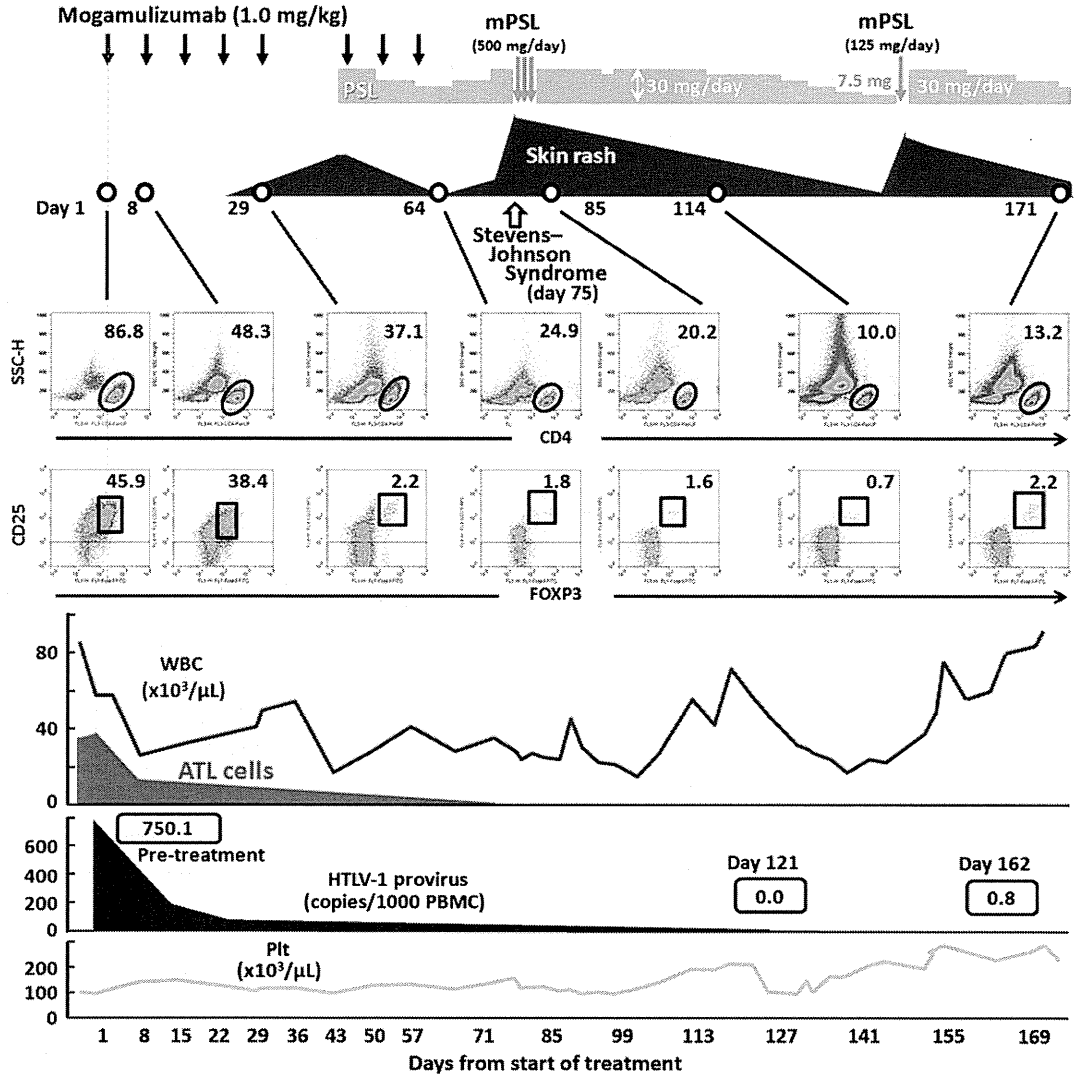

Fig. 1. Clinical course of an ATL patient receiving mogamulizumab monotherapy. ATL; adult T-cell leukemia/lymphoma; mPSL, methylprednisolone; Plt, platelet PSL; prednisolone; WBC, white blood cell.

load in asymptomatic carriers reported by other investigators is 18.0 copies/1000 cells.[6]

We also analyzed CD4, CD25 and FOXP3 expression by PBMC during and after antibody treatment (Fig. 1, middle panels). Before treatment, the majority of the patient's PBMC consisted of CD4-positive and CD25-positive ATL cells. Just before the 5th antibody infusion (day 29), around the time when her skin rash first appeared, the proportion of $CD25^{high}$-$FOXP3^{+}/CD4^{+}$ cells was markedly reduced, to 2.2%. This is low even compared to healthy individuals ($CD25^{high}$-$FOXP3^{+}/CD4^{+}$ cells, mean 3.3%, median 3.3%, range 2.6–4.4%) (Fig. 3). Around the time of SJS onset, the proportion of cells in the Treg subset was further reduced. The proportion of $CD25^{high}FOXP3^{+}/CD4^{+}$ cells at days 64, 85 and 114 was 1.8%, 1.6% and 0.7%, respectively. The striking reduction of the Treg subset persisted until 4 months after the last of the eight antibody infusions (day 171).

Discussion

Drugs often induce adverse cutaneous reactions of varying severity, ranging from simple uncomplicated eruptions to potentially fatal eruptions, such as SJS and TEN, within the spectrum of severe adverse reactions affecting skin and mucosa. Although many factors that might cause variability in the clinical course of such adverse reactions have been suggested, it remains unknown which factors are predominantly involved in these processes. The most prevalent severe drug eruptions are thought to be mediated by drug-reactive T-cells,[7] although we also need to be aware of the alternative view that severe drug eruptions are due to a dysregulated immune system. In this regard, an effect mediated by Treg cells is a likely candidate in severe drug eruptions. Indeed, it is reported that Treg cells can prevent experimentally-induced epidermal injury mimicking TEN in an animal model.[8] Furthermore, Takahashi *et al.* (2009) report that Treg cell function is profoundly impaired in patients with TEN.[9] Consistent with these reports, a marked reduction of the Treg subset was observed in the present case.

Mogamulizumab is the first therapeutic agent targeting CCR4, which is expressed on Treg cells,[10,11] to receive marketing approval anywhere in the world. The reduction of the Treg subset seen here was not specific to the present case, but is commonly observed in ATL patients receiving mogamulizumab. In fact, skin rashes were observed as a frequent non-hematologic adverse event (AE) (63%), mostly occurring

doi: 10.1111/cas.12116

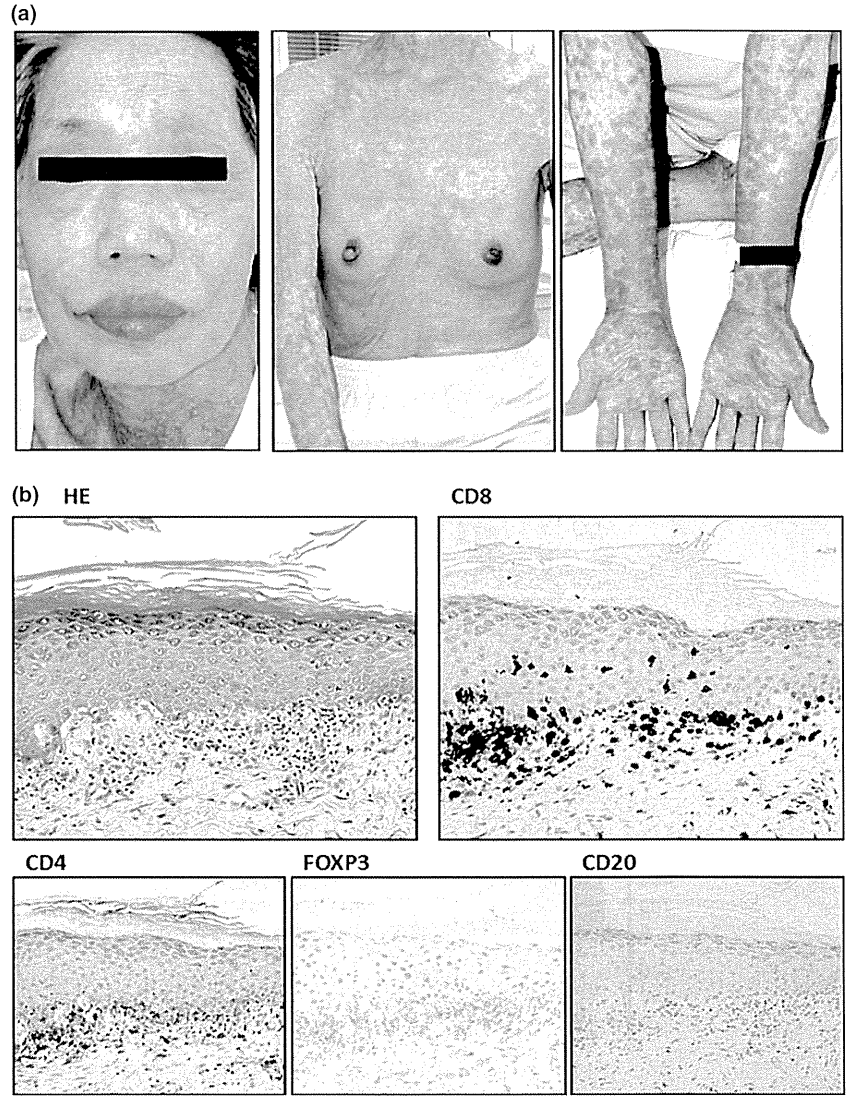

Fig. 2. (a) Macroscopic observations of the patient's skin on the day she was diagnosed with Stevens–Johnson Syndrome. (b) Corresponding skin biopsy showing liquefaction, degeneration and perivascular inflammation with dominant CD8-positive cells but almost no FOXP3-positive cells.

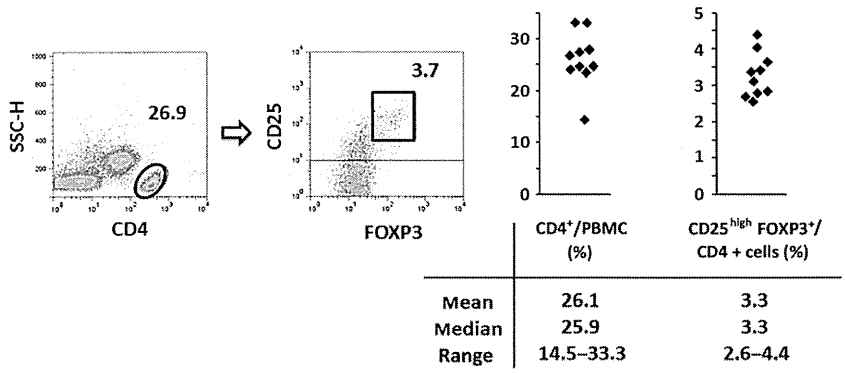

	$CD4^+$/PBMC (%)	$CD25^{high}$ $FOXP3^+$/ $CD4^+$ cells (%)
Mean	26.1	3.3
Median	25.9	3.3
Range	14.5–33.3	2.6–4.4

Fig. 3. $CD4^+CD25^{high}FOXP3^+$ regulatory T cells in PBMC from healthy volunteers (n = 10).

after the fourth or subsequent infusions in the phase II study.[4] The present case was one of these patients. It has been reported that alterations in $CD4^+CD25^+FOXP3^+$ Treg cell frequencies and/or function may contribute to various types of autoimmune diseases.[12] Because the CCR4 molecule aids lymphocyte skin-specific homing,[13] it is not unexpected that skin rashes, which could be an immune-related AE, will be frequently observed in ATL patients receiving mogamulizumab. Because it is an urgent issue to identify which factors determine the severity of immune-related skin disorders associated with mogamulizumab treatment, further investigation on this matter are clearly warranted.

However, reduction of Treg cells is a promising strategy for boosting antitumor immunity in cancer patients, because these cells are increased in the tumor microenvironment and may play an important role in tumor escape from host immunity in several different types of cancer.[14,15] Thus, reduction of Treg cells by mogamulizumab in cancer patients would have both potential benefits leading to enhanced antitumor immunity, but also pose risks of autoimmune disease. The skin-related SAE, including SJS/TEN, are representative of the latter. Currently, several clinical trials of mogamulizumab are being conducted worldwide, not only for ATL, but also other types of lymphoma. In addition, we are currently conducting a clinical trial of mogamulizumab for CCR4-negative solid cancers (UMIN000010050), specifically aiming to deplete Treg cells. Therefore, it is a matter of some urgency to establish the safest and most effective treatment strategies for using mogamulizumab not only in ATL patients but also other types of cancer, to maximize benefit and minimize risk.

In summary, the present case should contribute not only to our understanding of human pathology resulting from therapeutic depletion of Treg cells, but also alert us to the possibility of immune-related SAE, such as SJS/TEN, when using mogamulizumab.

Acknowledgments

The authors thank the husband of the patient for consenting to the publication of her clinical details. The present study was supported by Grants-in-Aid for Young Scientists (A) (No. 22689029), Scientific Research (B) (No. 22300333), and Scientific Support Programs for Cancer Research (No. 221S0001) from the Ministry of Education, Culture, Sports, Science and Technology of Japan, a Grant-in-Aid from the National Cancer Center Research and Development Fund (No. 23-A-17), and Health and Labour Sciences Research Grants (H22-Clinical Cancer Research-general-028 and H23-Third Term Comprehensive Control Research for Cancer-general-011) from the Ministry of Health, Labour and Welfare, Japan.

Disclosure Statement

Nagoya City University Graduate School of Medical Sciences has received research grant support from Kyowa Hakko Kirin for works provided by Takashi Ishida. Takashi Ishida received honoraria from Kyowa Hakko Kirin for his works. Shiro Akinaga is an employee of Kyowa Hakko Kirin. No other conflict of interest relevant to this article is reported.

References

1 Ishida T, Ueda R. Antibody therapy for Adult T-cell leukemia-lymphoma. *Int J Hematol* 2011; **94**: 443–52.
2 Ishii T, Ishida T, Utsunomiya A *et al.* Defucosylated humanized anti-CCR4 monoclonal antibody KW-0761 as a novel immunotherapeutic agent for adult T-cell leukemia/lymphoma. *Clin Cancer Res* 2010; **16**: 1520–31.
3 Yamamoto K, Utsunomiya A, Tobinai K *et al.* Phase I study of KW-0761, a defucosylated humanized anti-CCR4 antibody, in relapsed patients with adult T-cell leukemia-lymphoma and peripheral T-cell lymphoma. *J Clin Oncol* 2010; **28**: 1591–8.
4 Ishida T, Joh T, Uike N *et al.* Defucosylated anti-CCR4 monoclonal antibody (KW-0761) for relapsed adult T-cell leukemia-lymphoma: a multicenter phase ii study. *J Clin Oncol* 2012; **30**: 837–42.
5 Tsukasaki K, Utsunomiya A, Fukuda H *et al.* VCAP-AMP-VECP compared with biweekly CHOP for adult T-cell leukemia-lymphoma: Japan Clinical Oncology Group Study JCOG9801. *J Clin Oncol* 2007; **25**: 5458–64.
6 Sonoda J, Koriyama C, Yamamoto S *et al.* HTLV-1 provirus load in peripheral blood lymphocytes of HTLV-1 carriers is diminished by green tea drinking. *Cancer Sci* 2004; **95**: 596–601.
7 Nassif A, Bensussan A, Boumsell L *et al.* Toxic epidermal necrolysis: effector cells are drug-specific cytotoxic T cells. *J Allergy Clin Immunol* 2004; **114**: 1209–15.
8 Azukizawa H, Sano S, Kosaka H, Sumikawa Y, Itami S. Prevention of toxic epidermal necrolysis by regulatory T cells. *Eur J Immunol* 2005; **35**: 1722–30.
9 Takahashi R, Kano Y, Yamazaki Y, Kimishima M, Mizukawa Y, Shiohara T. Defective regulatory T cells in patients with severe drug eruptions: timing of the dysfunction is associated with the pathological phenotype and outcome. *J Immunol* 2009; **182**: 8071–9.
10 Iellem A, Mariani M, Lang R *et al.* Unique chemotactic response profile and specific expression of chemokine receptors CCR4 and CCR8 by CD4(+) CD25(+) regulatory T cells. *J Exp Med* 2001; **194**: 847–53.
11 Ishida T, Ishii T, Inagaki A *et al.* Specific recruitment of CC chemokine receptor 4-positive regulatory T cells in Hodgkin lymphoma fosters immune privilege. *Cancer Res* 2006; **66**: 5716–22.
12 Michels-van Amelsfort JM, Walter GJ, Taams LS. $CD4^+$ $CD25^+$ regulatory T cells in systemic sclerosis and other rheumatic diseases. *Expert Rev Clin Immunol* 2011; **7**: 499–514.
13 Campbell JJ, Haraldsen G, Pan J *et al.* The chemokine receptor CCR4 in vascular recognition by cutaneous but not intestinal memory T cells. *Nature* 1999; **400**: 776–80.
14 Jacobs JF, Nierkens S, Figdor CG, de Vries IJ, Adema GJ. Regulatory T cells in melanoma: the final hurdle towards effective immunotherapy? *Lancet Oncol* 2012; **13**: e32–42.
15 Ishida T, Ueda R. Immunopathogenesis of lymphoma: focus on CCR4. *Cancer Sci* 2011; **102**: 44–50.

doi: 10.1111/cas.12116

IJC
International Journal of Cancer

Induction of CD8 T-cell responses restricted to multiple HLA class I alleles in a cancer patient by immunization with a 20-mer NY-ESO-1f (NY-ESO-1 91-110) peptide

Shingo Eikawa[1,2], Kazuhiro Kakimi[3], Midori Isobe[2], Kiyotaka Kuzushima[4], Immanuel Luescher[5], Yoshihiro Ohue[2], Kazuhiro Ikeuchi[1], Akiko Uenaka[6], Hiroyoshi Nishikawa[7], Heiichiro Udono[1], Mikio Oka[2] and Eiichi Nakayama[6]

[1] Department of Immunology, Okayama University Graduate School of Medicine, Dentistry and Pharmaceutical Sciences, Okayama, Japan
[2] Department of Respiratory Medicine, Kawasaki Medical School, Kurashiki, Japan
[3] Department of Immunotherapeutics, University of Tokyo Hospital, Tokyo, Japan
[4] Department of Immunology, Aichi Cancer Center, Nagoya, Japan
[5] Ludwig Institute for Cancer Research, University of Lausanne, Epalinges, Switzerland
[6] Faculty of Health and Welfare, Kawasaki University of Medical Welfare, Kurashiki, Japan
[7] Department of Experimental Immunology, Immunology Frontier Research Center, Osaka University, Osaka, Japan

Immunogenicity of a long 20-mer NY-ESO-1f peptide vaccine was evaluated in a lung cancer patient TK-f01, immunized with the peptide with Picibanil OK-432 and Montanide ISA-51. We showed that internalization of the peptide was necessary to present CD8 T-cell epitopes on APC, contrasting with the direct presentation of the short epitope. CD8 T-cell responses restricted to all five HLA class I alleles were induced in the patient after the peptide vaccination. Clonal analysis showed that B*35:01 and B*52:01-restricted CD8 T-cell responses were the two dominant responses. The minimal epitopes recognized by A*24:02, B*35:01, B*52:01 and C*12:02-restricted CD8 T-cell clones were defined and peptide/HLA tetramers were produced. NY-ESO-1 91-101 on A*24:02, NY-ESO-1 92-102 on B*35:01, NY-ESO-1 96-104 on B*52:01 and NY-ESO-1 96-104 on C*12:02 were new epitopes first defined in this study. Identification of the A*24:02 epitope is highly relevant for studying the Japanese population because of its high expression frequency (60%). High affinity CD8 T-cells recognizing tumor cells naturally expressing the epitopes and matched HLA were induced at a significant level. The findings suggest the usefulness of a long 20-mer NY-ESO-1f peptide harboring multiple CD8 T-cell epitopes as an NY-ESO-1 vaccine. Characterization of CD8 T-cell responses in immunomonitoring using peptide/HLA tetramers revealed that multiple CD8 T-cell responses comprised the dominant response.

The NY-ESO-1 antigen was originally identified in esophageal cancer by serological expression cloning (SEREX) using autologous patient serum.[1,2] NY-ESO-1 expression is observed in a wide range of human malignancies, but the expression is restricted to germ cells in the testes in normal adult tissues.[1–4] Therefore, NY-ESO-1 has emerged as a prototype of a class of cancer/testis (CT) antigens.[5] The efficacy of the NY-ESO-1 antigen as a cancer vaccine has been studied extensively using various preparations, *e.g.*, peptide, protein or DNA, etc. of the antigen with various adjuvants.[6–14] These studies established the safety of the NY-ESO-1 vaccine and demonstrated its immunogenicity.

In a phase I clinical trial, we immunized cancer patients with a complex of cholesterol-bearing hydrophobized pullulan and NY-ESO-1 whole protein (CHP-NY-ESO-1) and showed that the vaccine had potent capacity to induce the NY-ESO-1 antibody in vaccinated patients.[13,14] The most dominant serological antigenic epitope was NY-ESO-1 91-108. The CHP-NY-ESO-1 vaccine also elicited CD4 and CD8 T-cell responses in immunized patients.[14] Analysis of T cell responses against overlapping peptides (OLPs) spanning the NY-ESO-1 molecule revealed that two dominant NY-ESO-1 regions, regions II (73-114) and III (121-144), were recognized by either CD4 or CD8 T-cells in most patients irrespective of their HLA type. Essentially similar findings were obtained by studies using other preparations of NY-ESO-1 protein vaccine.[11,12,15]

Key words: cancer vaccine, NY-ESO-1, long peptide, CD8 T-cell response
Additional Supporting Information may be found in the online version of this article.
This article was published online on 22 June 2012. An error was subsequently identified. This notice is included in the online and print versions to indicate that both have been corrected 21 November 2012.
Grant sponsor: Ministry of Education, Culture, Sports, Science and Technology of Japan (Grant-in-Aid for Scientific Research (B)), New Energy and Industrial Technology Development Organization (NEDO), Japan
DOI: 10.1002/ijc.27682
History: Received 11 Jan 2012; Accepted 1 Jun 2012; Online 22 Jun 2012
Correspondence to: Eiichi Nakayama, M.D., Faculty of Health and Welfare, Kawasaki University of Medical Welfare, 288 Matsushima, Kurashiki, Okayama 701-0193, Japan, Tel.: +81-86-462-1111 ext. 54954, Fax: +81-86-464-1109, E-mail: nakayama@mw.kawasaki-m.ac.jp

What's new?

An antigen called NY-ESO-1 is expressed by a wide range of human cancers, and has shown promise as a cancer vaccine. In this study, the authors studied a peptide derived from that antigen, and analyzed the cellular and molecular mechanisms that allow the peptide to provoke an immune response. They found that the peptide must be internalized by antigen-presenting cells (APCs) in order to yield T-cells that can attack tumours via the NY-ESO-1 antigen. These data increase our understanding of the requirements for an effective therapeutic cancer vaccine. (This section added after initial online publication.)

CD8 T-cells induced by immunization with NY-ESO-1 class I short epitope peptides have been shown to be of low affinity and do not recognize naturally processed NY-ESO-1 on tumor cells.[16] However, the advantage of synthetic long peptides over short peptides for use as vaccines has been reported.[17] Long peptides do not bind to MHC class I molecules directly, and require antigen processing by dendritic cells to be presented. Therefore, the use of long peptides prevents the antigen peptides from direct binding to MHC class I molecules on nonprofessional antigen-presenting cells (APC), which may cause transient activation and subsequent anergy of CTLs in the absence of appropriate costimulatory signals.[17–19] Based on these findings, we recently used a long peptide spanning a peptide region NY-ESO-1 91-110 (NY-ESO-1f peptide) which included the dominant serological antigenic epitope and overlapped one of the two dominant regions recognized by CD4 and CD8 T-cells for a vaccine in a clinical trial.[20] Ten patients received the NY-ESO-1f peptide vaccine. The NY-ESO-1f peptide vaccine was well tolerated and elicited humoral, CD4 and CD8 T-cell responses in immunized patients.

In this study, we demonstrated that internalization of the peptide was necessary to present CD8 T-cell epitopes on APC treated with the long 20-mer NY-ESO-1f peptide. Analysis of the CD8 T-cell response in an NY-ESO-1f peptide-immunized patient revealed occurrence of responses restricted to all five HLA class I alleles defined in the patient. The frequency of A*24:02, B*35:01, B*52:01, C*03:03 and C*12:02-restricted CD8 T-cells in PBMCs was defined by clonal analysis revealing B*35:01- and B*52:01-restricted CD8 T-cell responses as dominant. By establishing clones from those HLA-restricted CD8 T-cells, new epitopes on A*24:02, B*35:01, B*52:01 and C*12:02 were defined and peptide/HLA tetramers were prepared. Clonal analysis showed that CD8 T-cells that recognize natural epitopes on tumor cells were induced in a significant proportion by immunization with the NY-ESO-1f peptide. Immunomonitoring using the tetramers revealed that multiple CD8 T-cell responses comprised the dominant response.

Material and Methods

Clinical trial

A phase I clinical trial of the NY-ESO-1f peptide vaccine was conducted to evaluate the safety, immune response and tumor response.[20] Patients with advanced cancers that were refractory to standard therapy and expressed NY-ESO-1 as assessed by immunohistochemistry (IHC) were eligible. The protocol was approved by the Ethics Committee of Tokyo, Osaka and Okayama Universities in light of the Declaration of Helsinki. Written informed consent was obtained from each patient before enrolling in the study. The study was performed in compliance with Good Clinical Practice. The study was registered in the University hospital Medical Information Network Clinical Trials Registry (UMIN-CTR) Clinical Trial (Unique trial number: UMIN000001260) on July 24, 2008 (UMIN-CTRURL: http://www.umin.ac.jp/ctr/ index.htm).

Blood samples

Patient TK-f01 was a lung cancer patient who received a right middle lobectomy in October, 2004.[20] As the tumor continued to grow despite chemotherapy, he was enrolled in the study in June, 2008. The patient received 12 vaccinations once every 3 weeks. Peripheral blood was drawn from patient TK-f01 with informed consent for immunological monitoring. Peripheral blood mononuclear cells (PBMCs) were isolated from heparinized blood by density gradient centrifugation using a Histopaque 1077 (Sigma-Aldrich, St. Louis, MO). CD4-, CD8- and CD19-positive cells were purified by magnetic cell sorting (Miltenyi Biotec, Bergisch Gladbach, Germany). The residual cells were kept for use as APC. The cells were stored in liquid N_2 until use. HLA tying was done with PBMCs by a sequence-specific oligonucleotide probe and sequence-specific priming of genomic cDNA using a standard procedure.

Cell lines

LC99A and OU-LC-OK are lung cancer cell lines. SK-OV3 is an ovarian cancer cell line and SK-MEL37 is a melanoma cell line. These cell lines were kept by serial passage in tissue culture. EBV-B cells were generated from CD19-positive peripheral blood B cells using a culture supernatant from EBV-producing B95-8 cells. The medium used to maintain these cell lines was RPMI1640 supplemented with 10% FCS (JRM, Bioscience, Lenexa, KA), 2 mmol/l Glutamax, antibitotics, and 10 mmol/l HEPES (Invitrogen, Carlsbad, CA).

Antibodies

Anti-human CD4, anti-human CD8, anti-HLA class I and anti-HLA class II mAbs were purchased from BD Bioscience (San Jose, CA).

Peptides

The following series of 28 18-mer OLPs and a C-terminal 30-mer peptide spanning the entire NY-ESO-1 protein were used: 18.1 (1-18), 18.2 (7-24), 18.3 (13-30), 18.4 (19-36), 18.5 (25-42), 18.6 (31- 48), 18.7 (37-54), 18.8 (43-60), 18.9 (49-